Elettra Sincrotrone Trieste

ATOMIC FORCE MICROSCOPY
Imaging in Biology
Membranes

Membranes

▶ FIGURE 5-4 The faces of cellular membranes. The plasma membrane, a single bilayer membrane, encloses the cell. In this highly schematic representation, internal cytosol (green stipple) and external environment (purple) define the cytosolic (red) and exoplasmic (black) faces of the bilayer. Vesicles and some organelles have a single membrane and their internal aqueous space (purple) is topologically equivalent to the outside of the cell. Three organelles—the nucleus, mitochondrion, and chloroplast (which is not shown)—are enclosed by two membranes separated by a small intermembrane space. The exoplasmic faces of the inner and outer membranes around these organelles border the intermembrane space between them. For simplicity, the hydrophobic membrane interior is not indicated in this diagram.

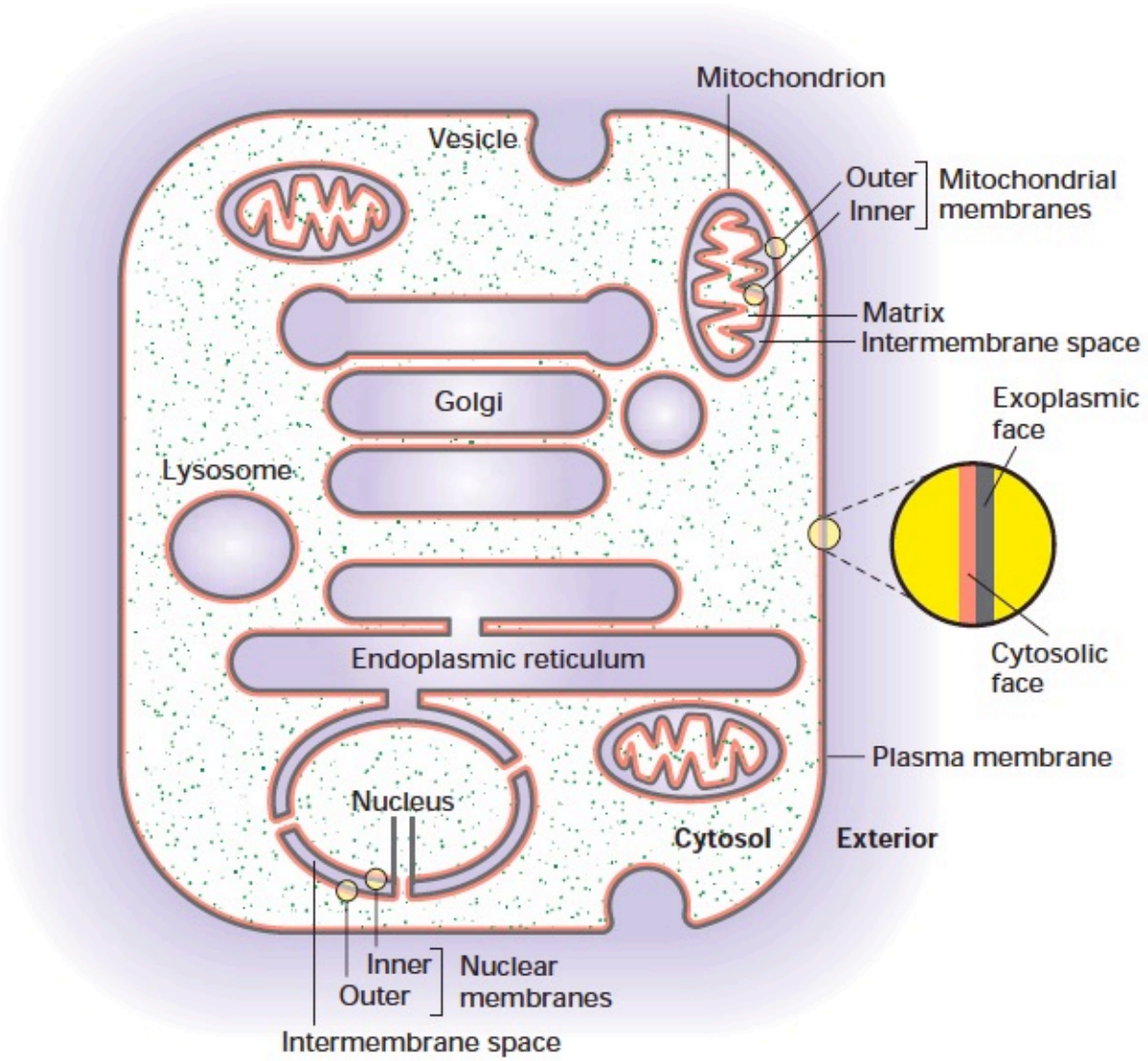

Lipids

Water insoluble compounds (soluble in organic solvents)

Biological role:

- energy supply
- energy store
- components of cellular and organelle membranes

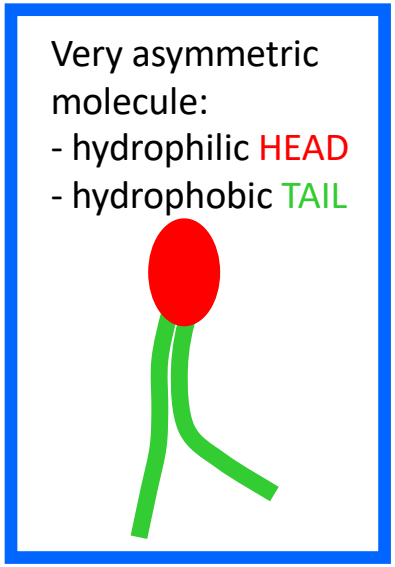

When in aqueous environment the heads have affinity for the water molecules, while the tails tend to avoid water by sticking together.

micelle

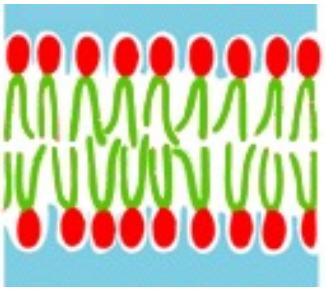

lipid bilayer

Fatty acids

Carboxylic acids with long hydrocarbon chains (12-24 -CH_2- units)

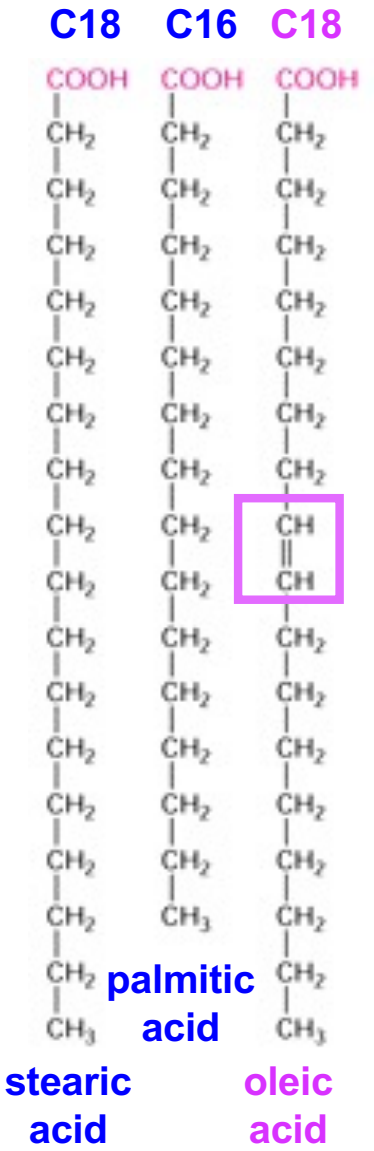

Some have one or more double bonds and are called unsaturated. The double bond is rigid and creates a kink in the chain; the rest of the chain is free to rotate

Stearic acid - saturated

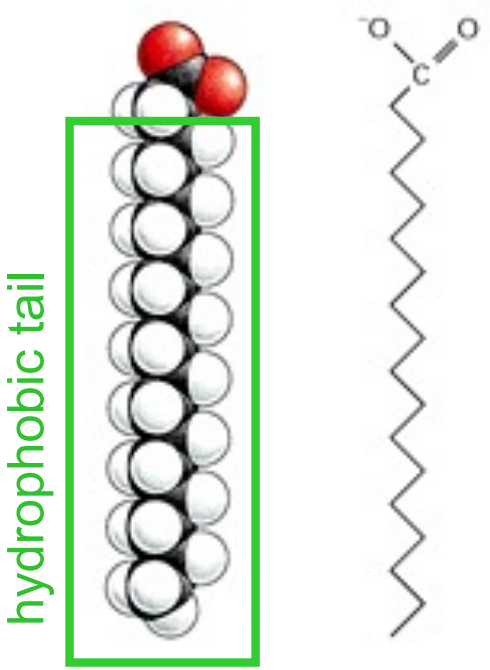

Oleic acid - unsaturated

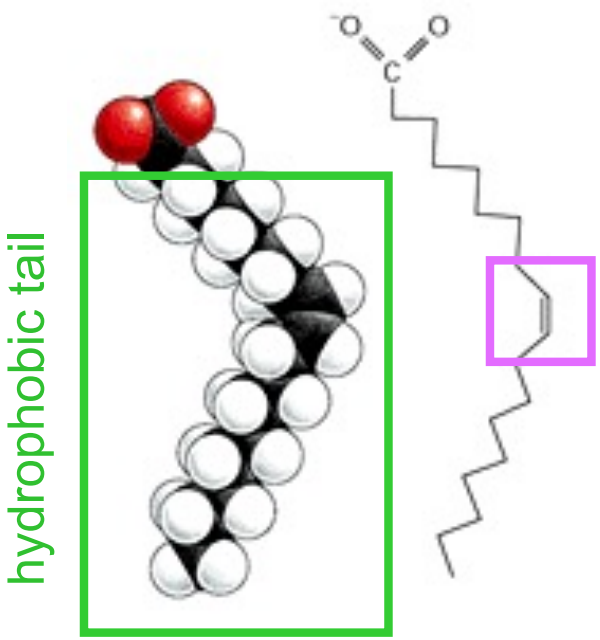

Fatty acids are used as E storage

To ensure a continuous supply of fuel for oxidative metabolism, animal cells store glucose in the form of glycogen and fatty acids in the form of fats.

A fat molecule is composed of three molecules of fatty acid linked to glycerol: triacylglycerols (*triglycerides*).

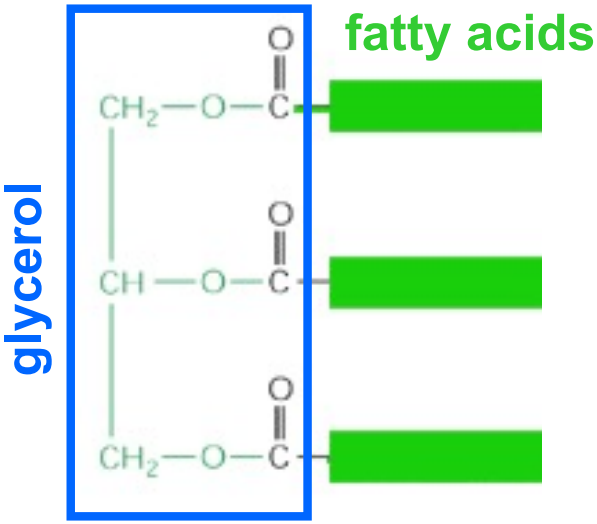

Fat is a far more important storage form than Glycogen (glucose polymer), because its oxidation releases more than six times as much energy.

Triglycerides have no charge and are virtually insoluble in water, coalescing into droplets in the cytosol of adipose cells.

fat droplet

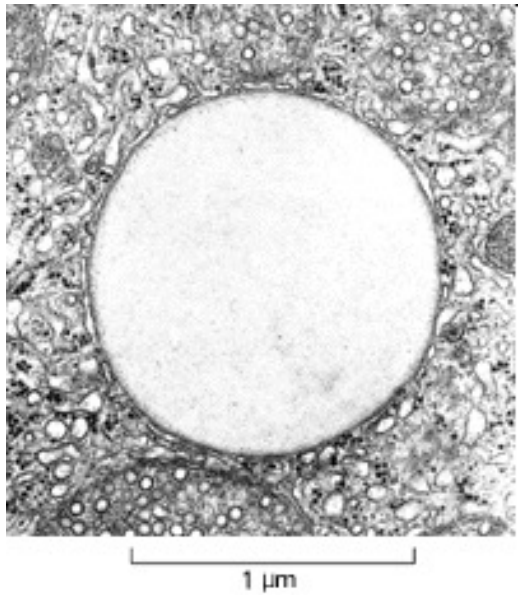

Phospholipids

In phospholipids, two of the OH groups of glycerol are linked to fatty acids, while the third is linked to a phosphate group, which can be further linked to a polar group such as choline, serine, inositol, etc...

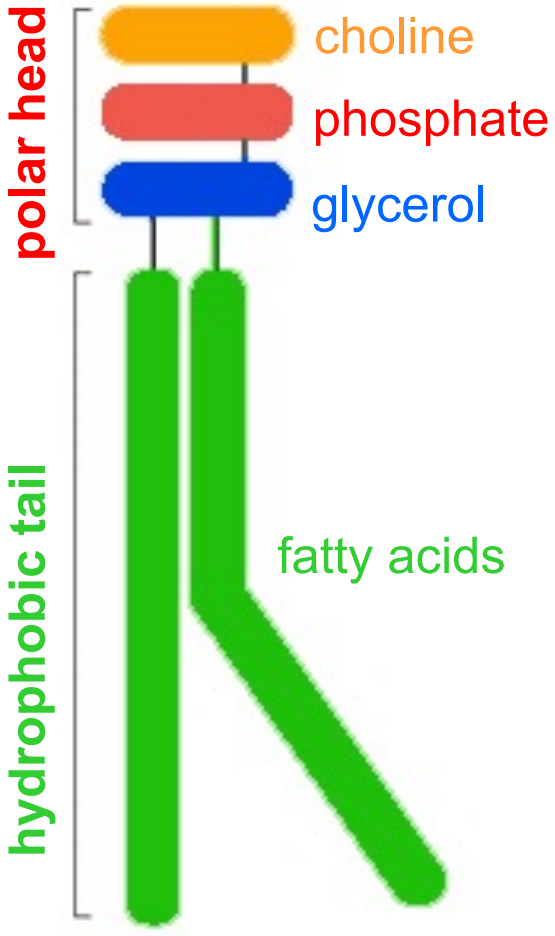

Very asymmetric molecule:
- hydrophilic HEAD
- hydrophobic TAIL

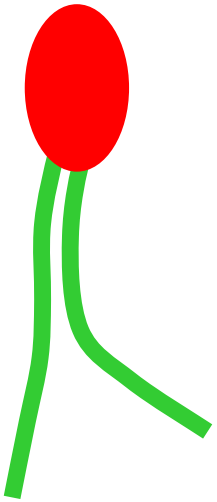

Phospholipids and membranes

Phospholipids are the major constituent of cell membranes.

When in aqueous environment the heads have affinity for the water molecules, while the tails tend to avoid water by sticking together.

Cellular membranes are essentially made up by phospholipid bilayers.

micelle

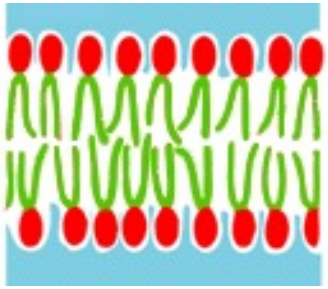

lipid bilayer

Phospholipid mobility

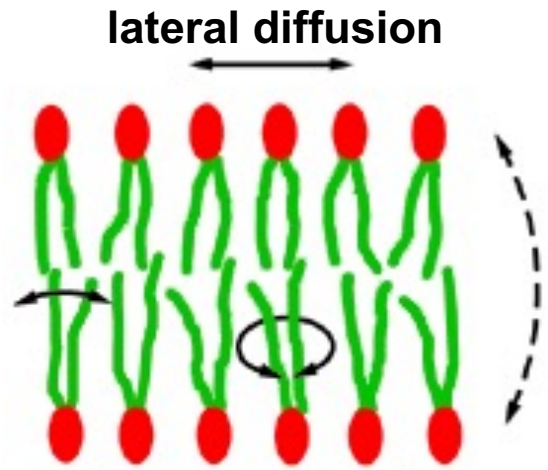

Saturated vs unsaturated lipids

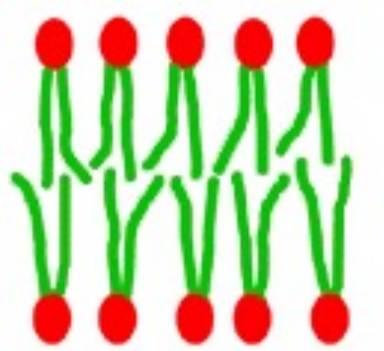

unsaturated, more difficult to pack, more fluid

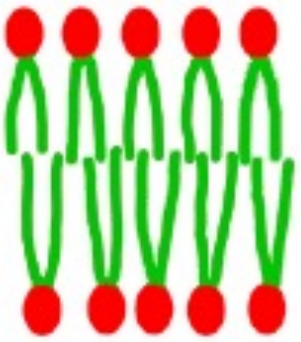

saturated, easier to pack, less fluid

Sphingolipids

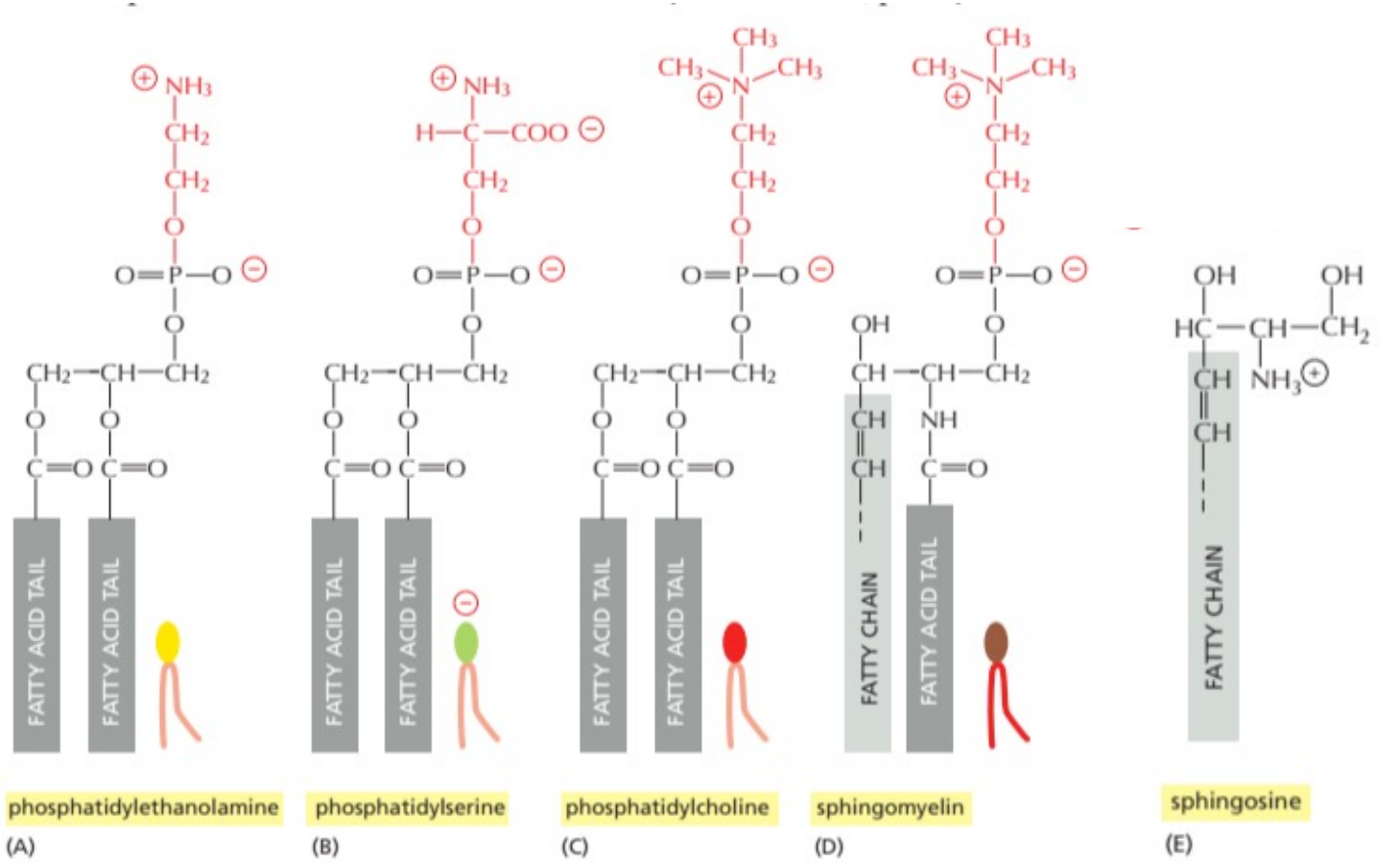

Sphingolipids are derivatives of sphingosine (red), an amino alcohol with a long hydrocarbon chain.
Various fatty acyl chains are connected to sphingosine by an amide bond.
The sphingomyelins (SM), which contain a phosphocholine head group, are phospholipids.
Other sphingolipids are glycolipids in which a single sugar residue or branched oligosaccharide is attached to the sphingosine backbone.

Cholesterol and steroids

Steroids (such as cholesterol) have a rigid structure made up by 4 rings.

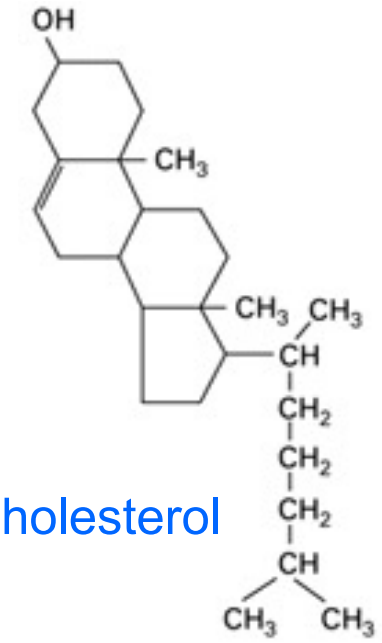

Cholesterol

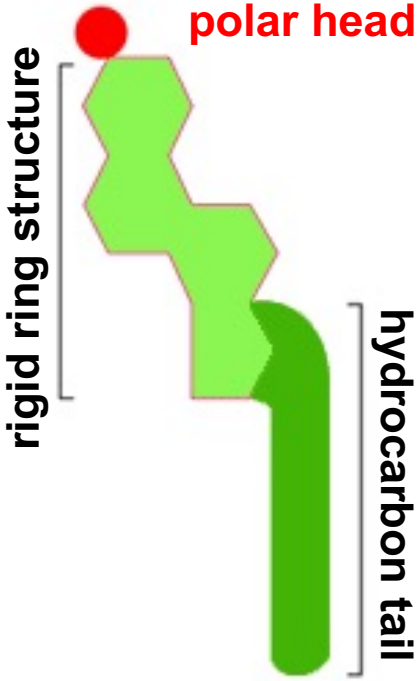

Other important steroid are the sex hormones, such as testosterone and estrogen:

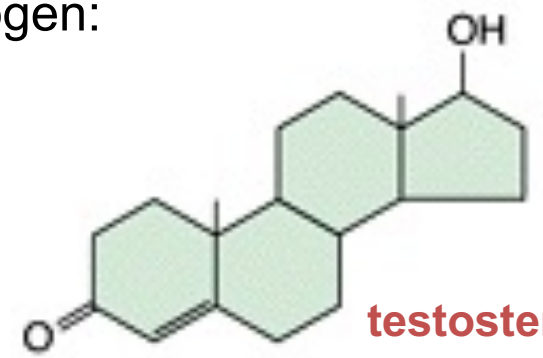

testosterone

Cholesterol is an important component of the eukaryotic membranes and has a key role in controlling the membrane fluidity.

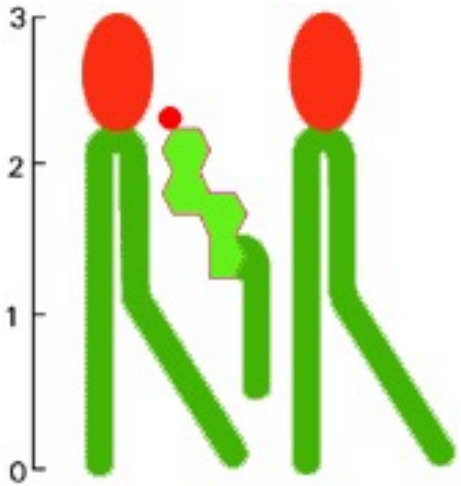

Cell membranes

Membranes are made of strongly anisotropic molecules
Strongly anisotropic molecules like to self-organizing.

•a typical eukaryotic cell membrane contains 500–2000 different lipid species

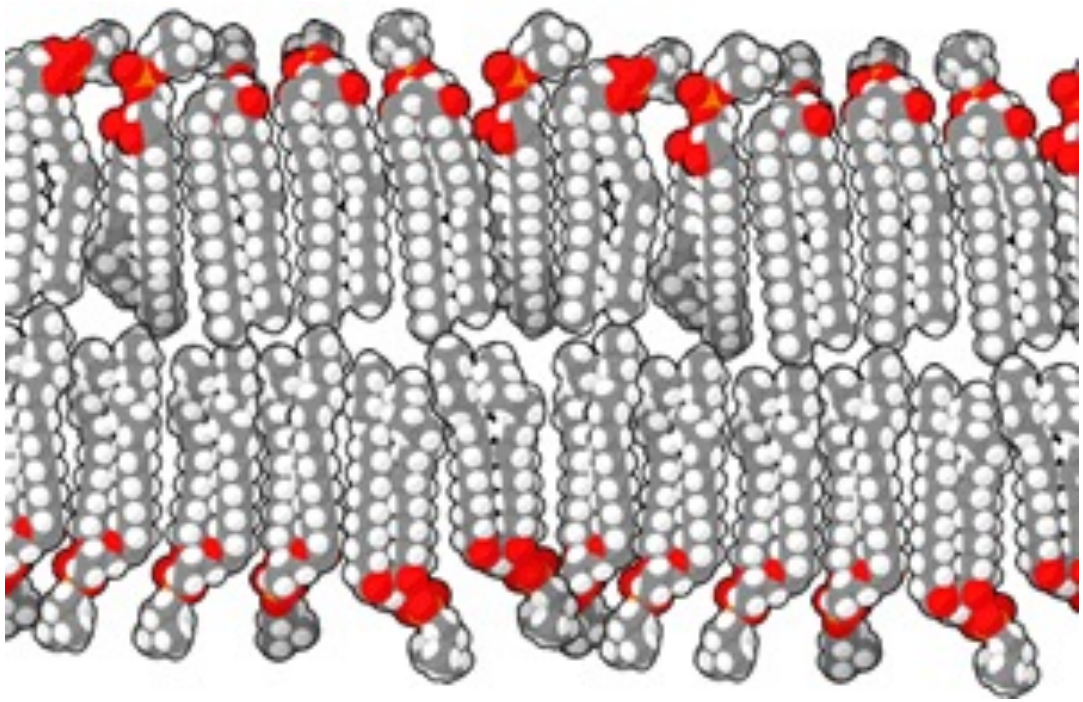

The Lipid Bilayer Is a Two-dimensional Fluid

Around 1970, researchers first recognized that individual lipid molecules are able to diffuse freely within the plane of a lipid bilayer. The initial demonstration came from studies of synthetic (artificial) lipid bilayers, which can be made in the form of spherical vesicles, called **liposomes** (**Figure 10–9**); or in the form of planar bilayers formed across a hole in a partition between two aqueous compartments or on a solid support.

Various techniques have been used to measure the motion of individual lipid molecules and their components. One can construct a lipid molecule, for example, with a fluorescent dye or a small gold particle attached to its polar head group and follow the diffusion of even individual molecules in a membrane. Alternatively, one can modify a lipid head group to carry a "spin label," such as a nitroxide

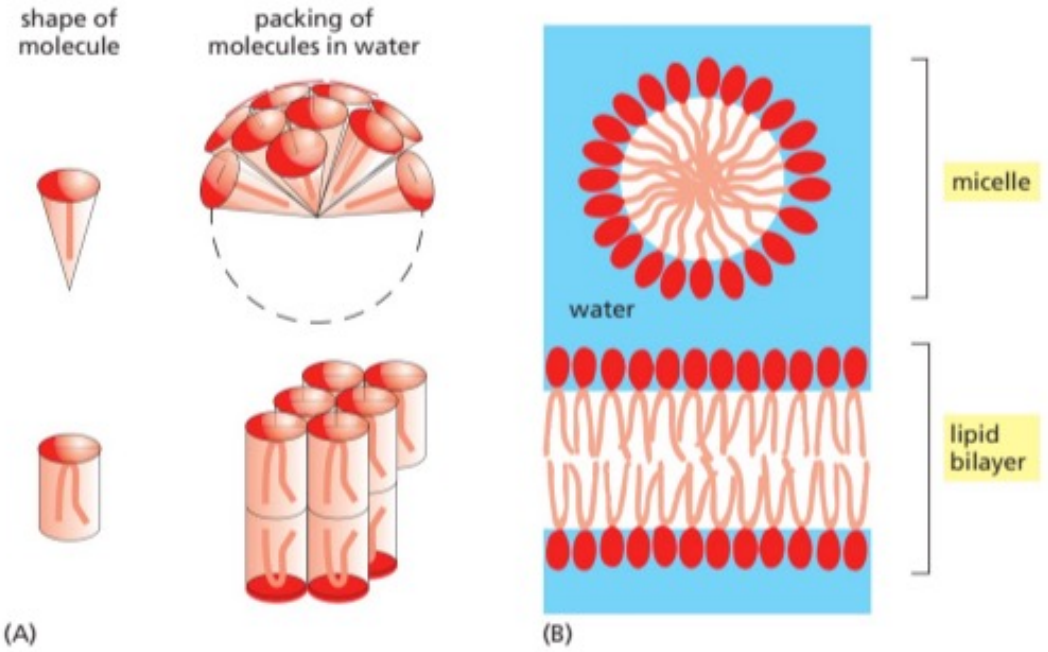

Figure 10–7 Packing arrangements of amphiphilic molecules in an aqueous environment. (A) These molecules spontaneously form micelles or bilayers in water, depending on their shape. Cone-shaped amphiphilic molecules *(above)* form micelles, whereas cylinder-shaped amphiphilic molecules such as phospholipids *(below)* form bilayers. (B) A micelle and a lipid bilayer seen in cross section. Note that micelles of amphiphilic molecules are thought to be much more irregular than drawn here (see Figure 10–26C).

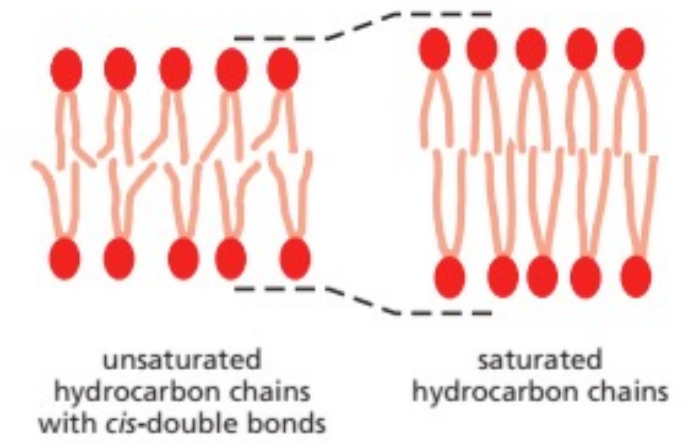

Figure 10–11 The influence of *cis*-double bonds in hydrocarbon chains. The double bonds make it more difficult to pack the chains together, thereby making the lipid bilayer more difficult to freeze. In addition, because the hydrocarbon chains of unsaturated lipids are more spread apart, lipid bilayers containing them are thinner than bilayers formed exclusively from saturated lipids.

Bacteria, yeasts, and other organisms whose temperature fluctuates with that of their environment adjust the fatty acid composition of their membrane lipids to maintain a relatively constant fluidity. As the temperature falls, for instance, the cells of those organisms synthesize fatty acids with more cis-double bonds, thereby avoiding the decrease in bilayer fluidity that would otherwise result from the temperature drop.

The fluidity of a lipid bilayer depends on both its composition and its temperature, as is readily demonstrated in studies of synthetic lipid bilayers. A synthetic bilayer made from a single type of phospholipid changes from a liquid state to a two-dimensional rigid crystalline (or gel) state at a characteristic temperature. This change of state is called a **phase transition**, and the temperature at which it occurs is lower (that is, the membrane becomes more difficult to freeze) if the hydrocarbon chains are short or have double bonds. A shorter chain length reduces the tendency of the hydrocarbon tails to interact with one another, in both the same and opposite monolayer, and cis-double bonds produce kinks in the chains that make them more difficult to pack together, so that the membrane remains fluid at lower temperatures

Alberts, Bruce; Molecular Biology of the Cell (p. 571). W. W. Norton & Company.

Cholesterol is an important component of the eukaryotic membranes and has a key role in controlling the membrane fluidity.

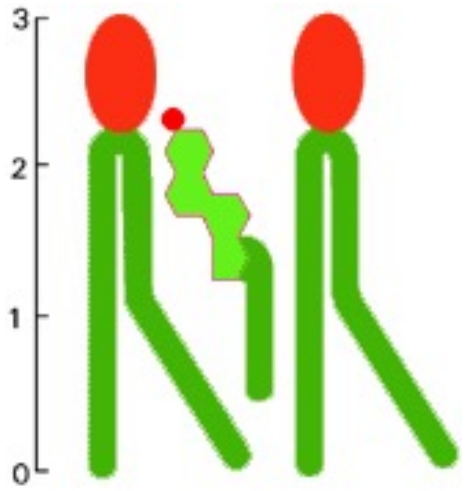

Cholesterol inserts into the bilayer with its hydroxyl group close to the polar head groups of the phospholipids, so that its rigid, platelike steroid rings interact with— and partly immobilize—those regions of the hydrocarbon chains closest to the polar head groups. By decreasing the mobility of the first few CH2 groups of the chains of the phospholipid molecules, cholesterol makes the lipid bilayer less deformable in this region and thereby decreases the permeability of the bilayer to small water-soluble molecules. Although cholesterol tightens the packing of the lipids in a bilayer, it does not make membranes any less fluid. At the high concentrations found in most eukaryotic plasma membranes, cholesterol also prevents the hydrocarbon chains from coming together and crystallizing.

Cell membranes

- biological membranes are fluid
- the fluidity is controlled by the % of saturated/unsaturated fatty acid and the % of cholesterol
- membranes are impermeable to ions and most polar molecules (H_2O is actively transported in)
- many proteins are embedded in the membrane
- the membrane is highly asymmetric

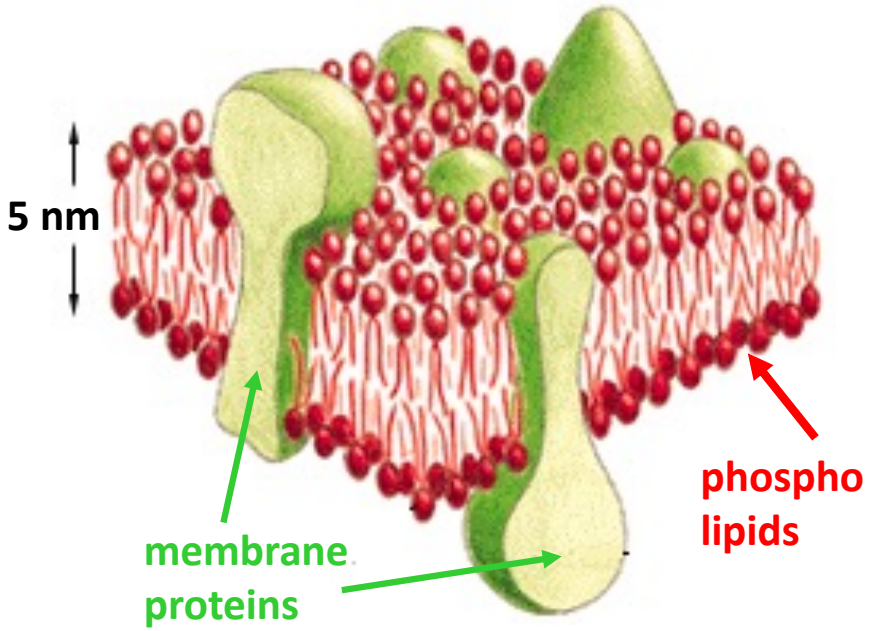

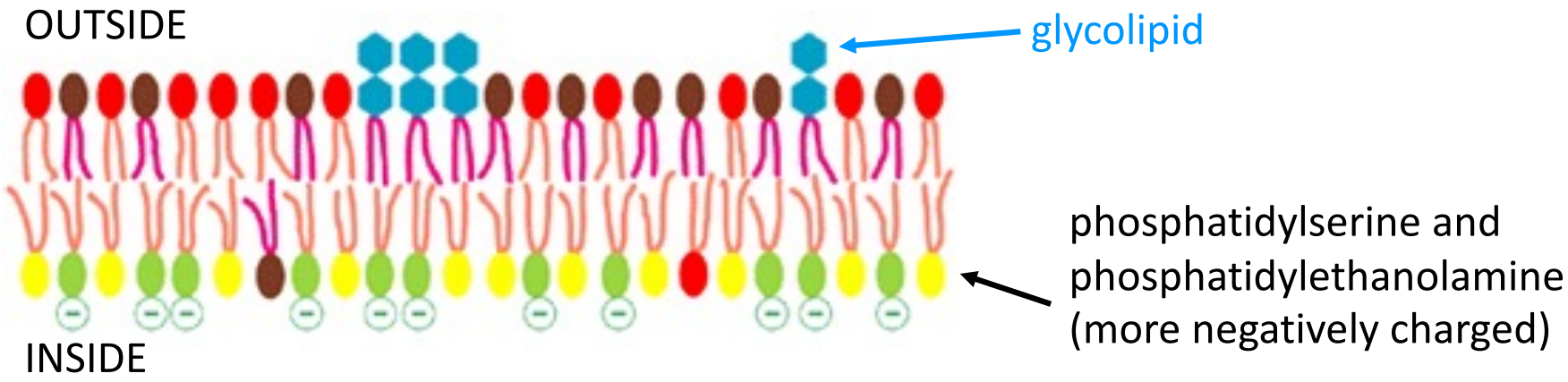

Cell membrane: an optimized 2D fluid system

Membrane fluidity depends on the type of lipid:
Saturated lipid are more ordered, therefore mode rigid then the **unsaturated** ones

Stearic acid - saturated

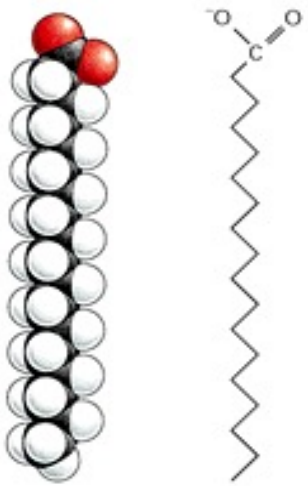

Oleic acid - unsaturated

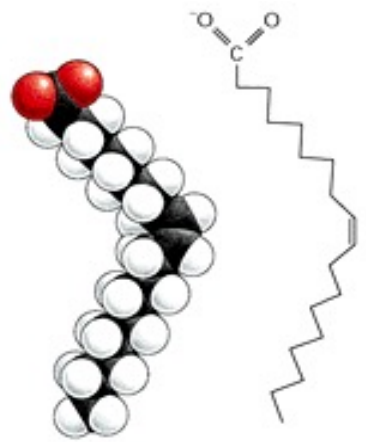

Phospholipid

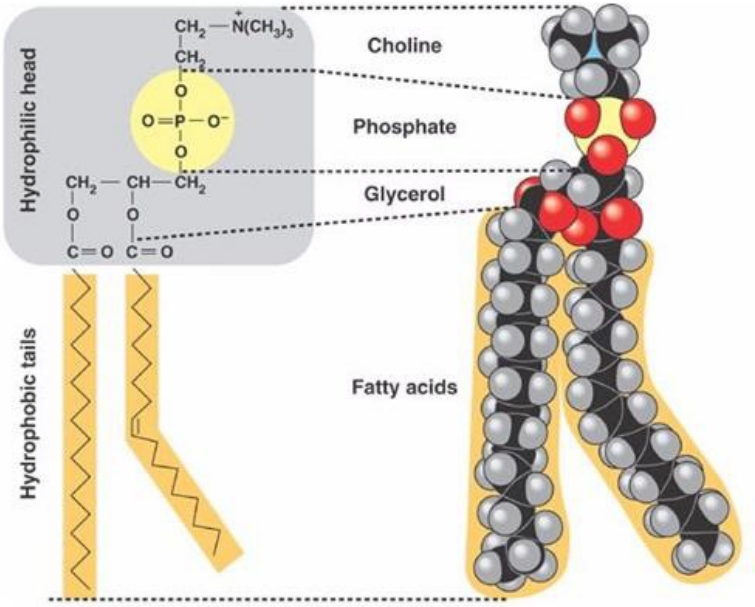

Saturated vs unsaturated lipids

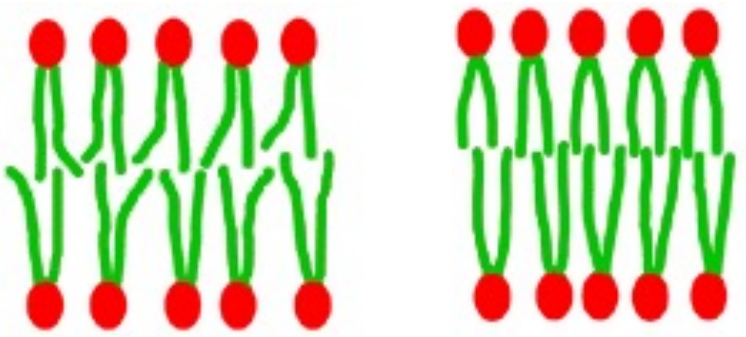

unsaturated, more difficult to pack, more fluid

saturated, easier to pack, less fluid

Membrane proteins

1. The residues accessible to lipid tails tend to be more hydrophobic than the residues buried inside the protein
2. Charged or polar residues can be exposed to the lipids, but they will interact either with the lipids head-groups or with other polar or charged residues of the protein
3. Polar aromatic residues (Trp, Tyr) can also interact with lipids, but tend to be located in the polar-apolar interfacial region, near the lipids carbonyls, and act as anchor for the protein in the bilayer

Examples:
the outer membrane proteins, the photosynthetic membrane proteins, the membrane transporters and channels, the respiratory enzymes, and the receptors and related proteins.

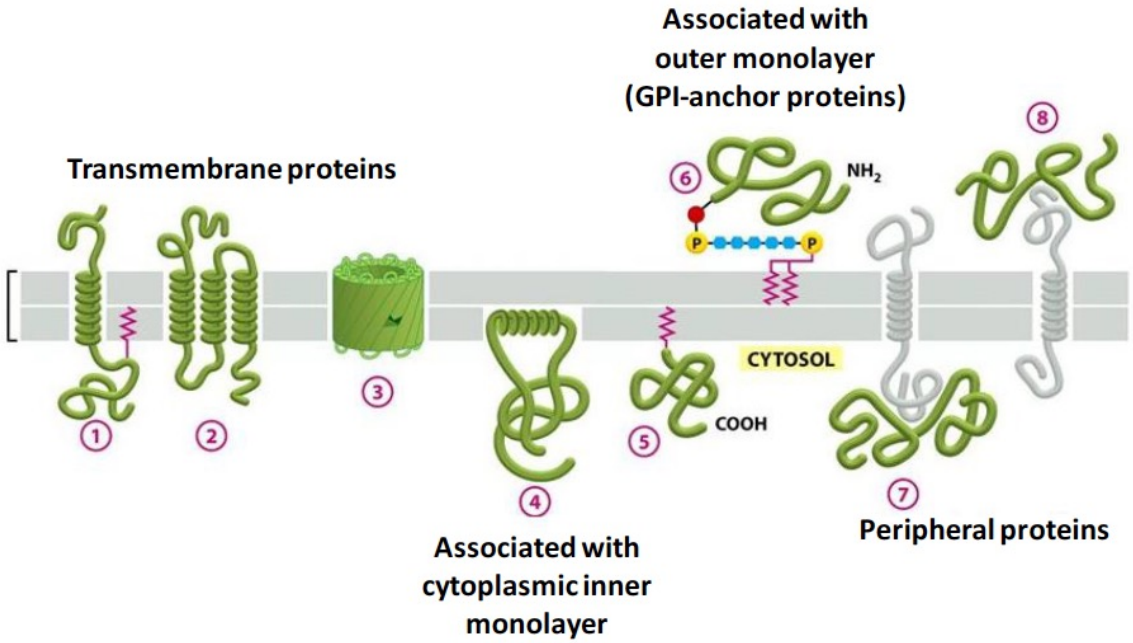

Cell membranes-rafts

Tasks such as energy transduction and chemical communication between the inside and the outside of the cell are achieved by membrane proteins. However, molecular level understanding of membrane proteins function is largely hindered by the lack of structural information available, especially in biologically relevant environments

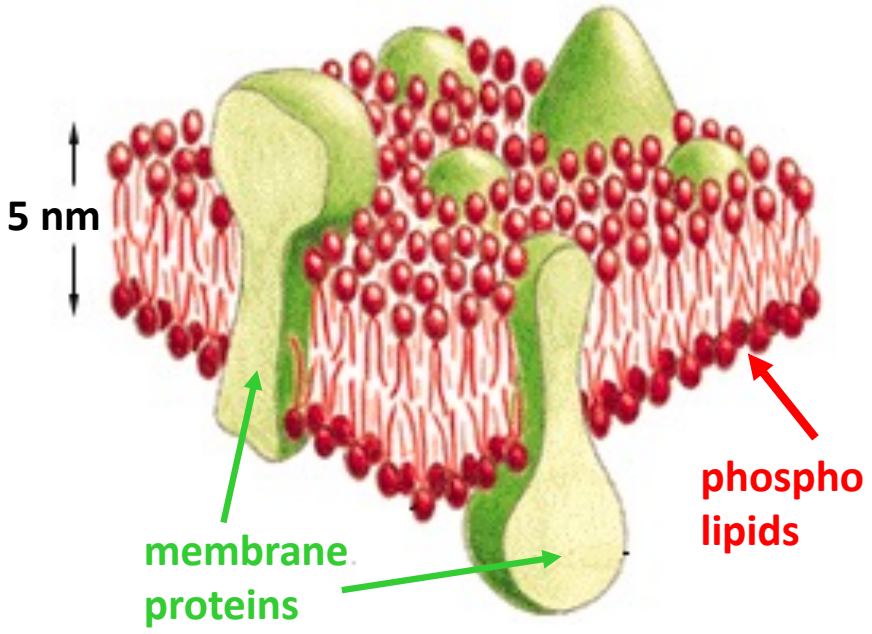

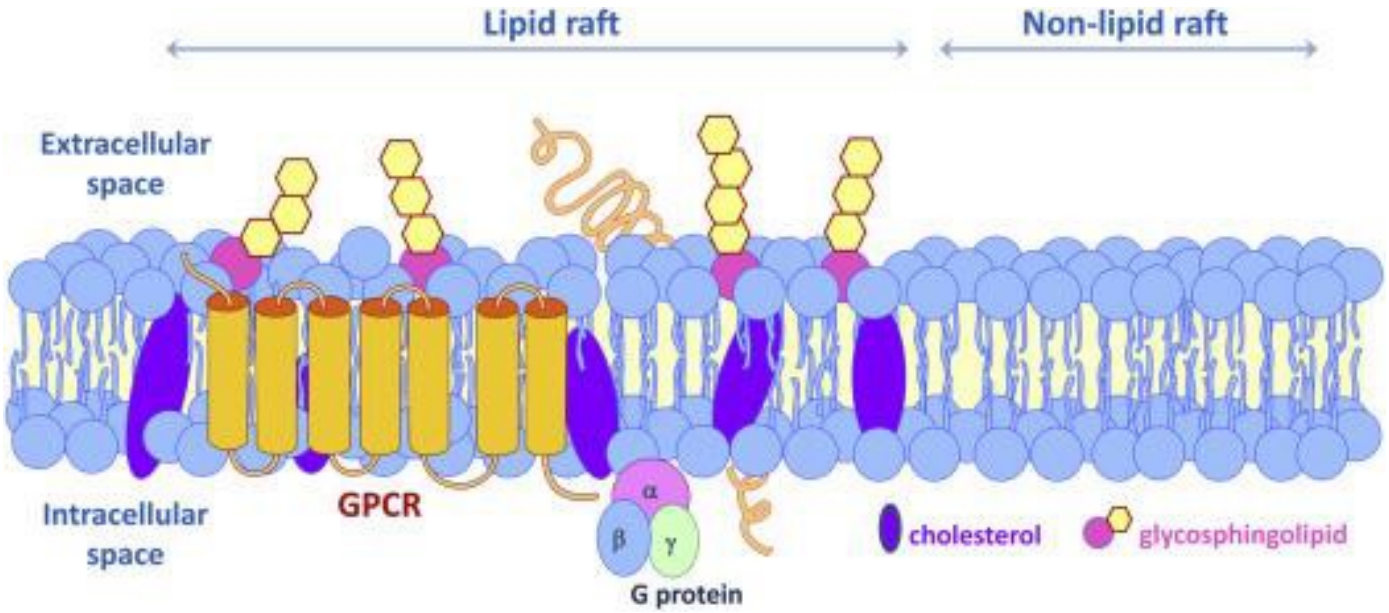

Model membranes

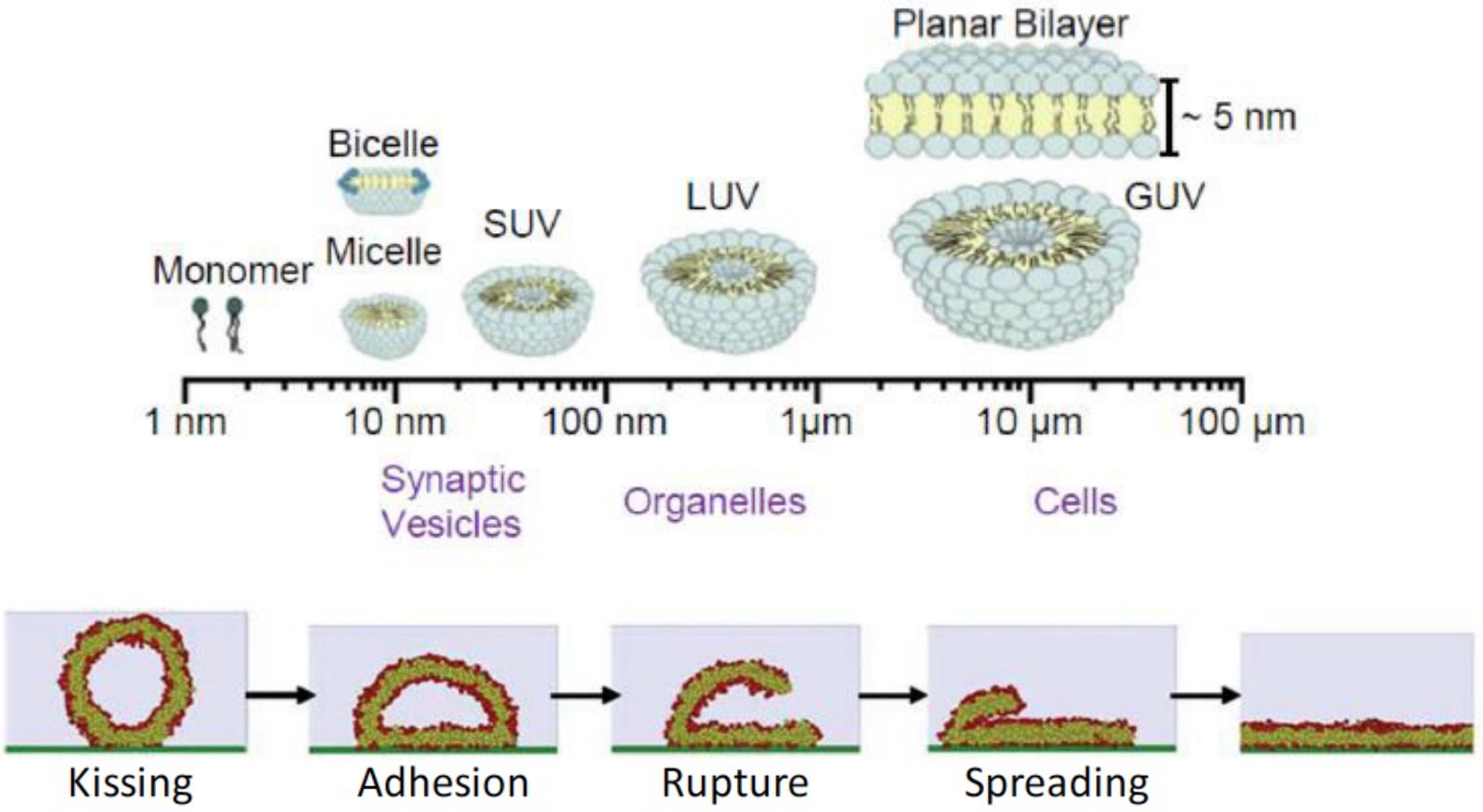

Cell membrane: an optimized 2D fluid system

Membrane fluidity depends on the type of lipid:

Saturated lipid are more ordered, therefore mode rigid then the **unsaturated** ones

Cholesterol is hydrophobic, but reacts with a OH^- group with the hydrophilic heads of neighbor phospholipids

Low T: chol is a spacer, fluidity high

High T: chol stabilizes the membrane (sealing)

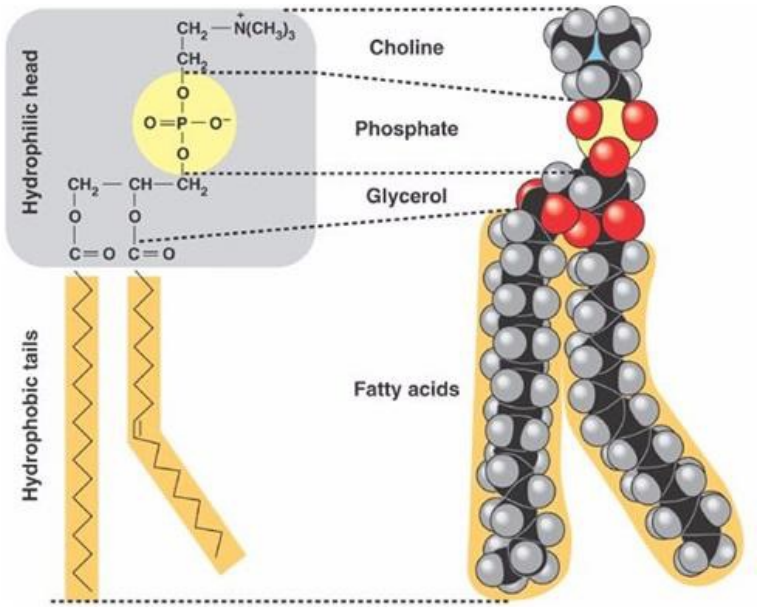

Stearic acid - saturated

Oleic acid - unsaturated

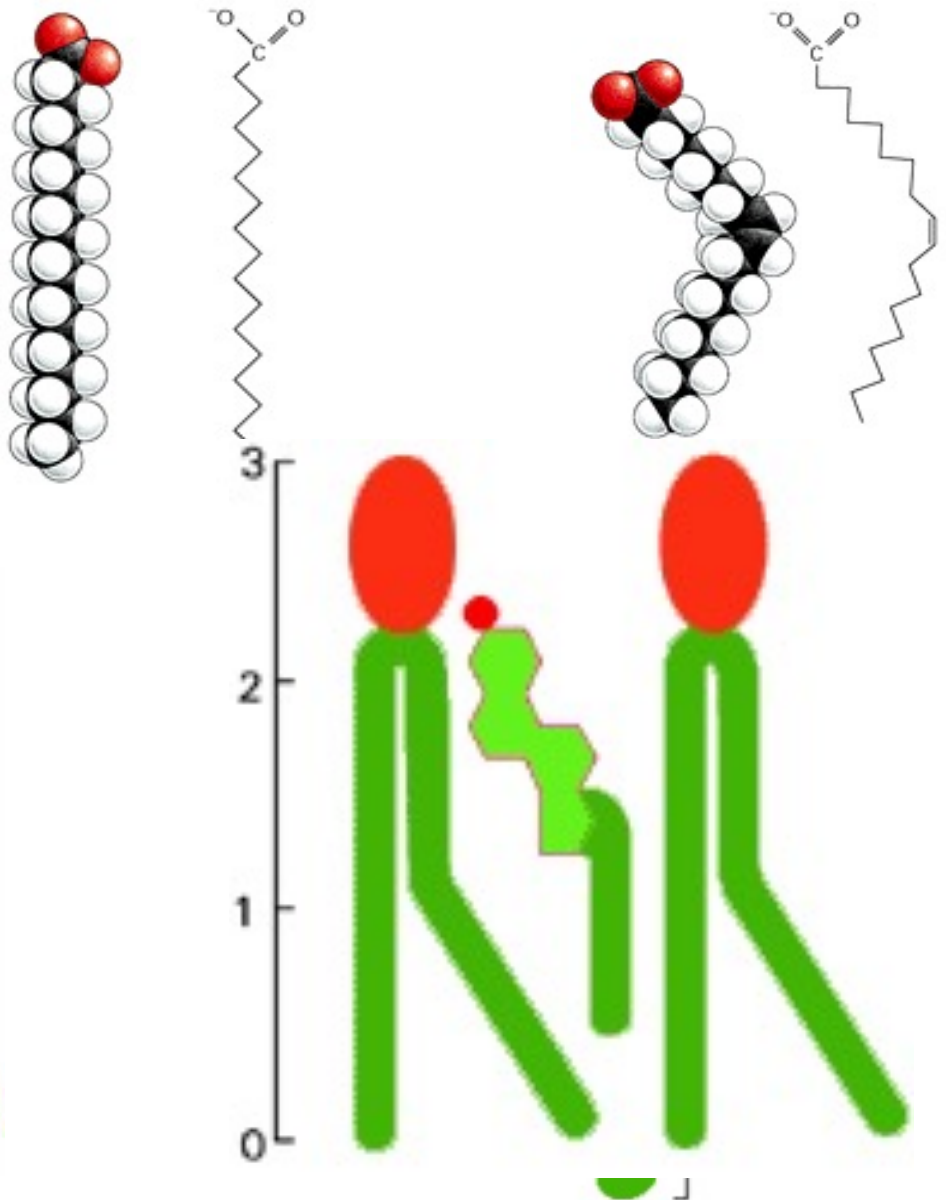

Study of unstructured protein oligomerization

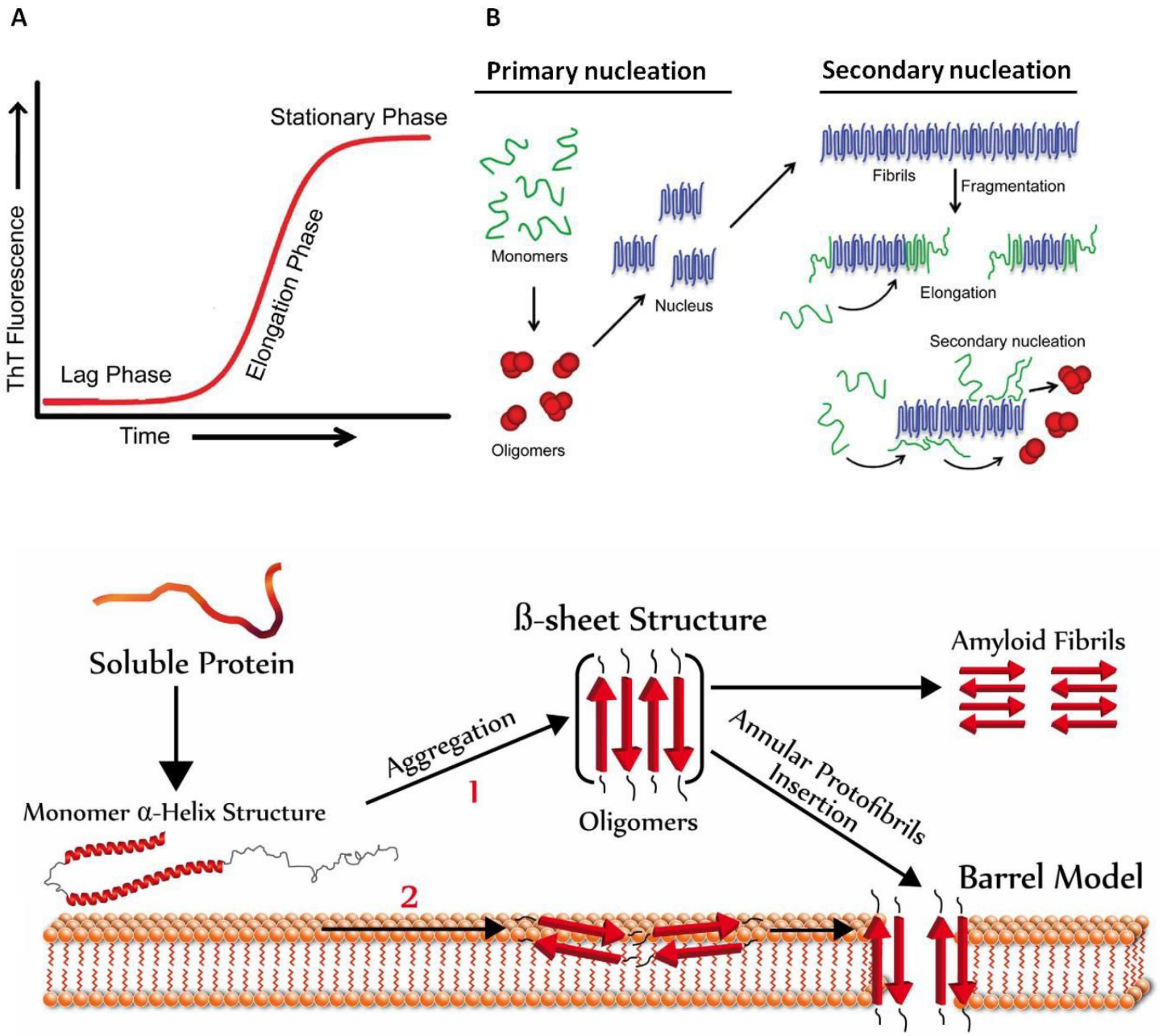

Multicomponent lipid membranes

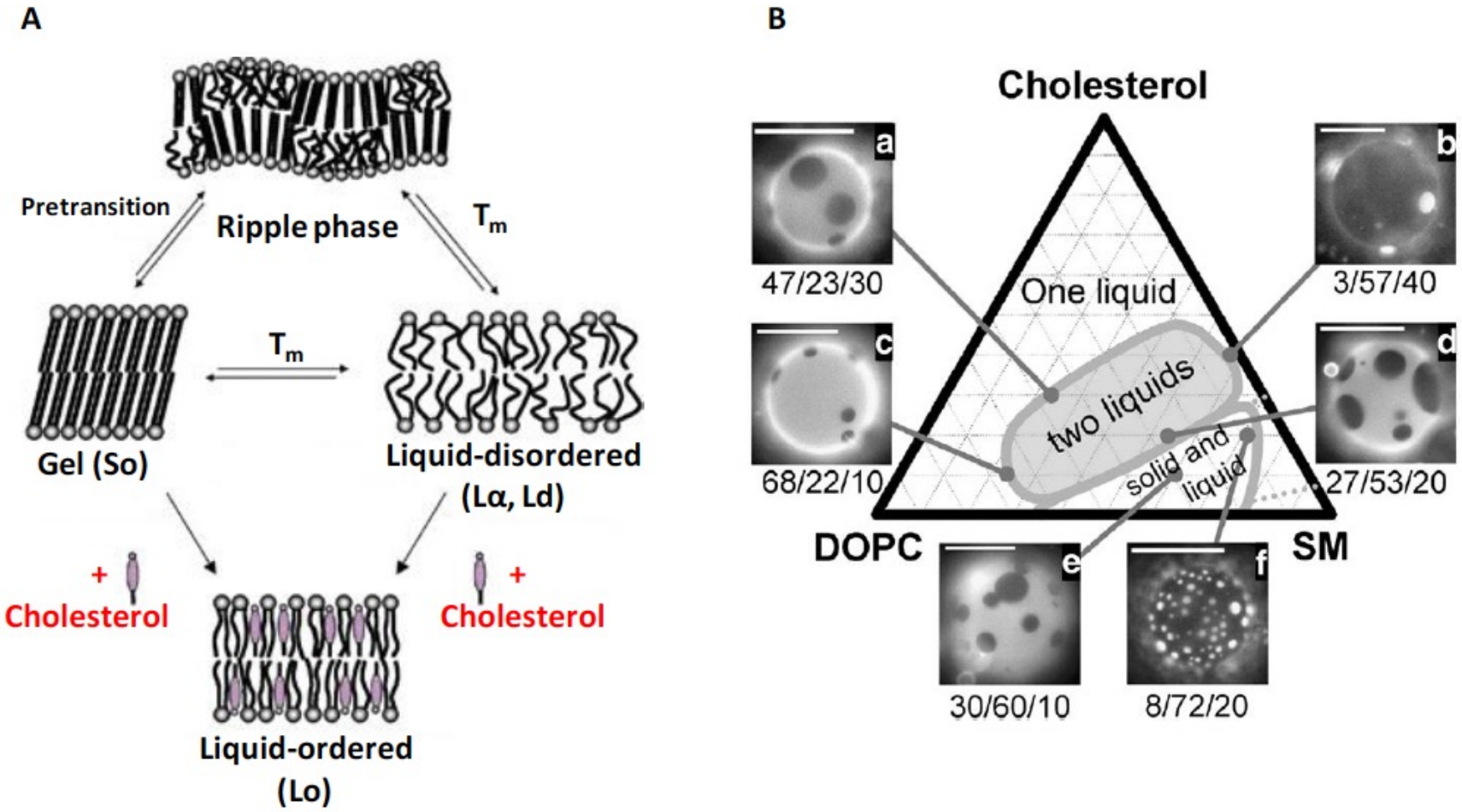

Model cell membranes-rafts

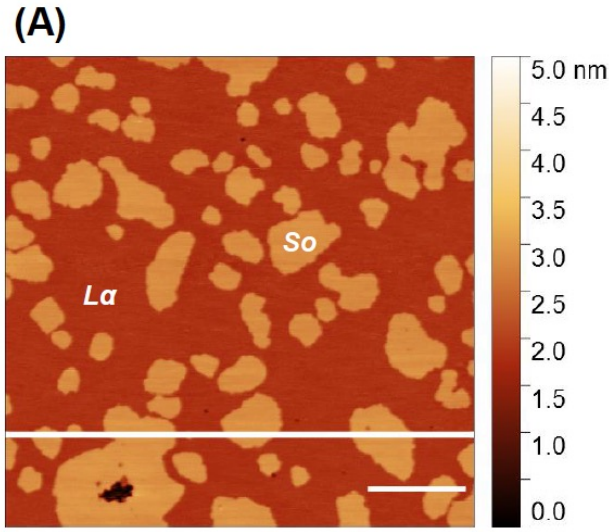

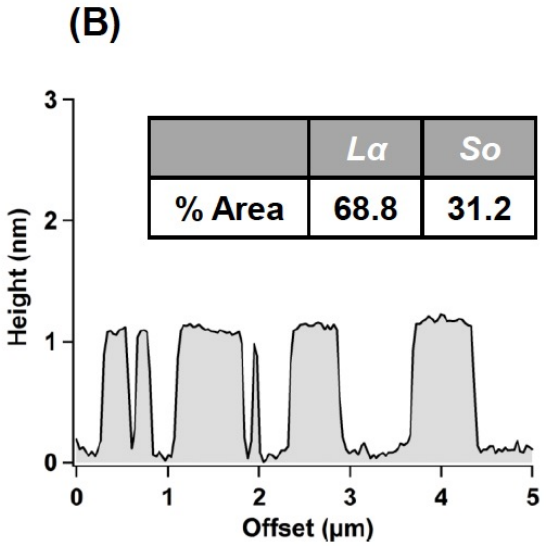

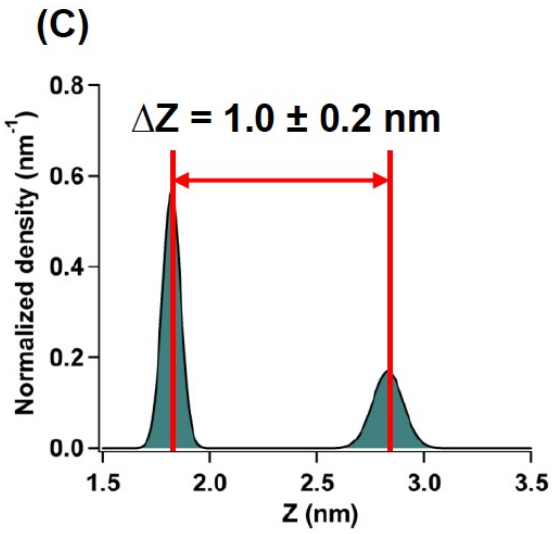

Coexistence of liquid-disordered (*Lα*) and solid-ordered (*So*) phase in planar supported lipid bilayer mimicking raft-like domains.

(A) AFM topography image of ternary SLB composed by DOPC, SM and cholesterol (66:33 +5% Chol). Image was taken in aqueous buffer in dynamic AC-mode. Scale bar: 1.0 μm. **(B)** Section analysis (white line in (A)) shows So-domains protruding from the fluid matrix (Lα) of SLB of ≈ 1.0 nm. **(C)** The height distribution graph

Model membranes-rafts

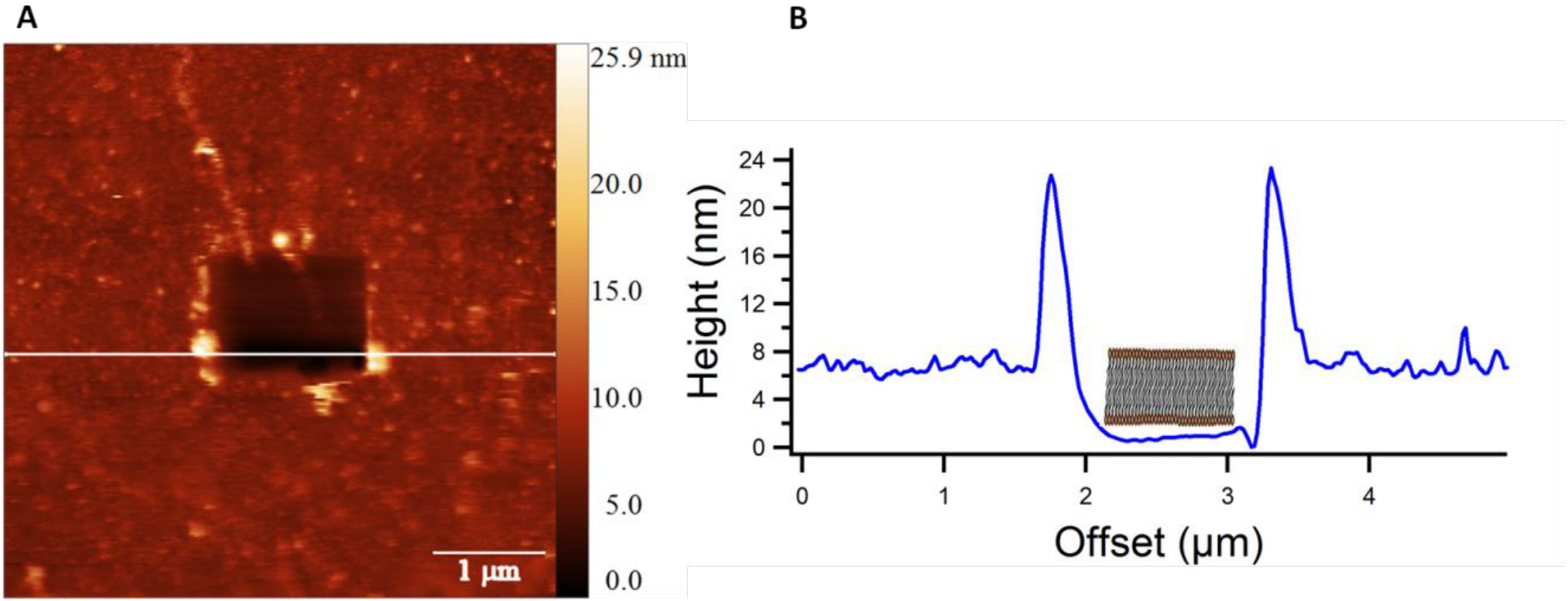

DOPC/SM (66:33)

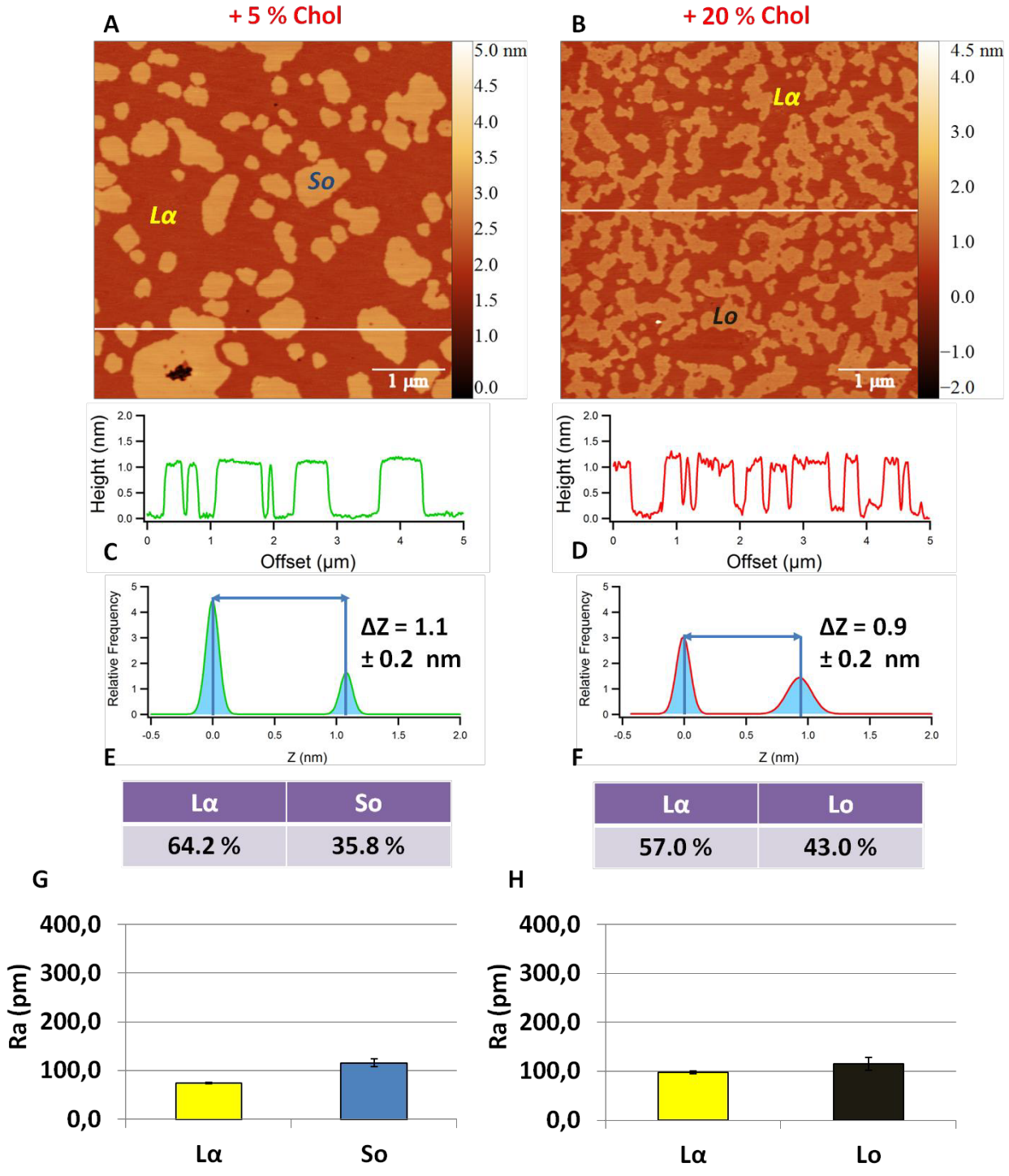
A
+ 5 % Chol
Lα
So
1 µm
5.0 nm
4.5
4.0
3.5
3.0
2.5
2.0
1.5
1.0
0.0
B
+ 20 % Chol
Lα
Lo
1 µm
4.5 nm
4.0
3.0
2.0
1.0
0.0
−1.0
−2.0
Height (nm)
Offset (µm)
C
D
Relative Frequency
Z (nm)
ΔZ = 1.1
± 0.2 nm
ΔZ = 0.9
± 0.2 nm
E
F
Lα
So
64.2 %
35.8 %
Lα
Lo
57.0 %
43.0 %
G
H
Ra (pm)
400,0
300,0
200,0
100,0
0,0
Lα
So
Lα
Lo

Membrane proteins

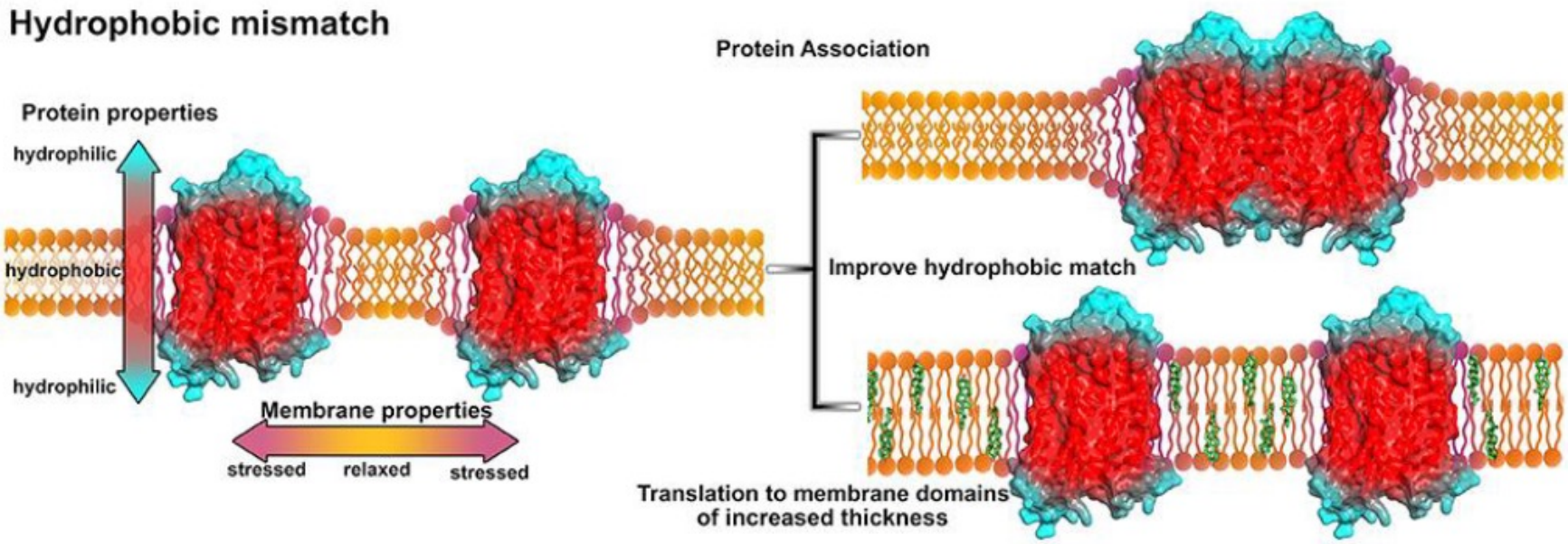

Lipid-protein interactions are very important for the stabilization of protein structure, regulation of protein activity and for partition of proteins in different lipid domains, as in lipid rafts. At the molecular level, these interactions drive the complex organization of plasma membrane.

Membrane proteins: **Lipidated-Prion protein (PrPC)**

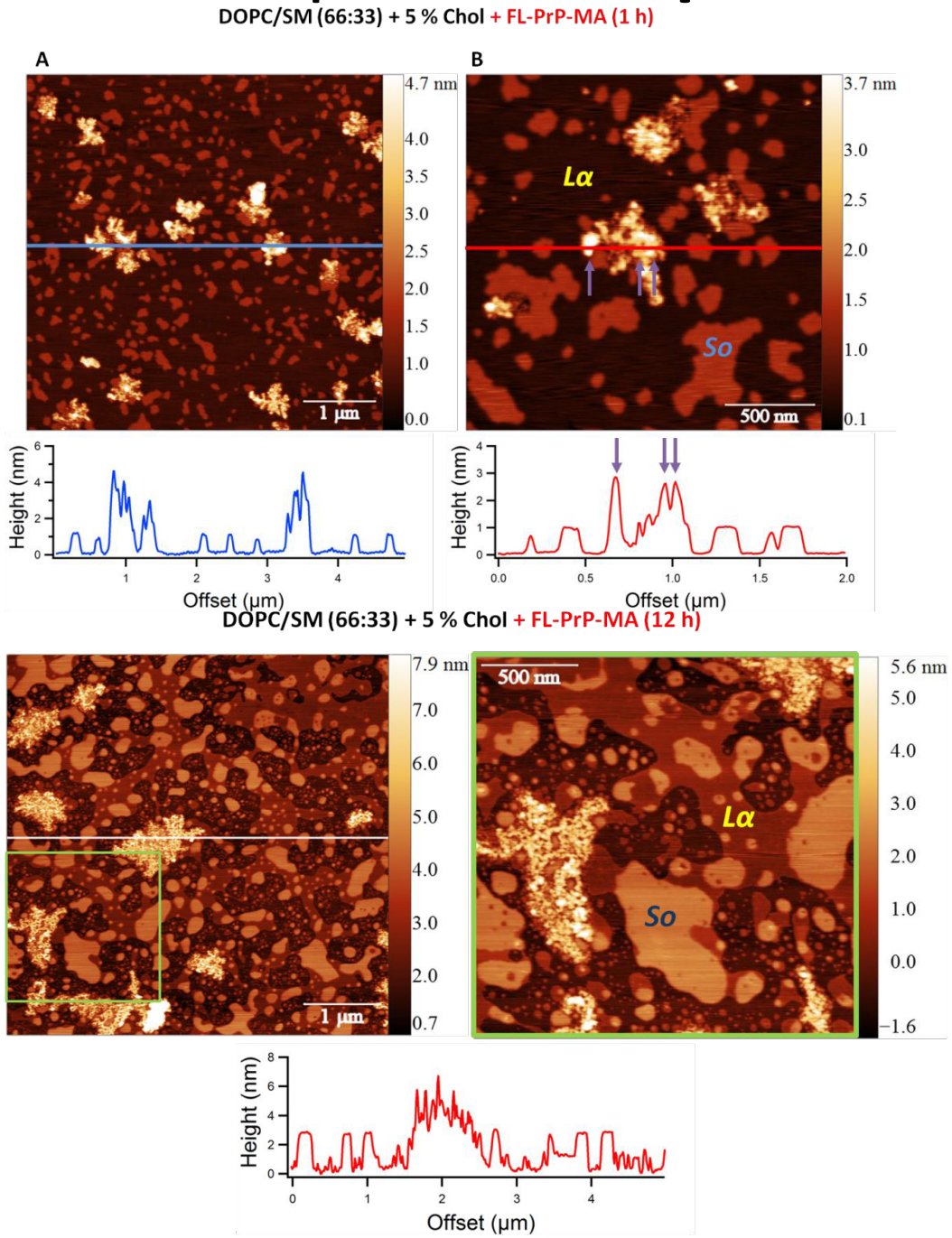

FL-PrPC-MA interacts with lipid raft domains without affecting the fluid phase of the bilayer. This could be due to the MA activity, which targets the protein to the ordered islands of membrane. However, formation of aggregated protein clusters which resemble oligomer accumulation are observed.

Membrane proteins: **Iron-mediated Alpha Synuclein (αS) aggregation**

Iron is implicated in the electron transfer during cellular respiration and as cofactor in the catalysis of enzymatic reactions.

Iron is potentially toxic when is present at high concentrations in the cell. It has been demonstrated that the total amount of iron increases physiologically in the brain with age and that this fact could be correlated with the old-age onset of PD

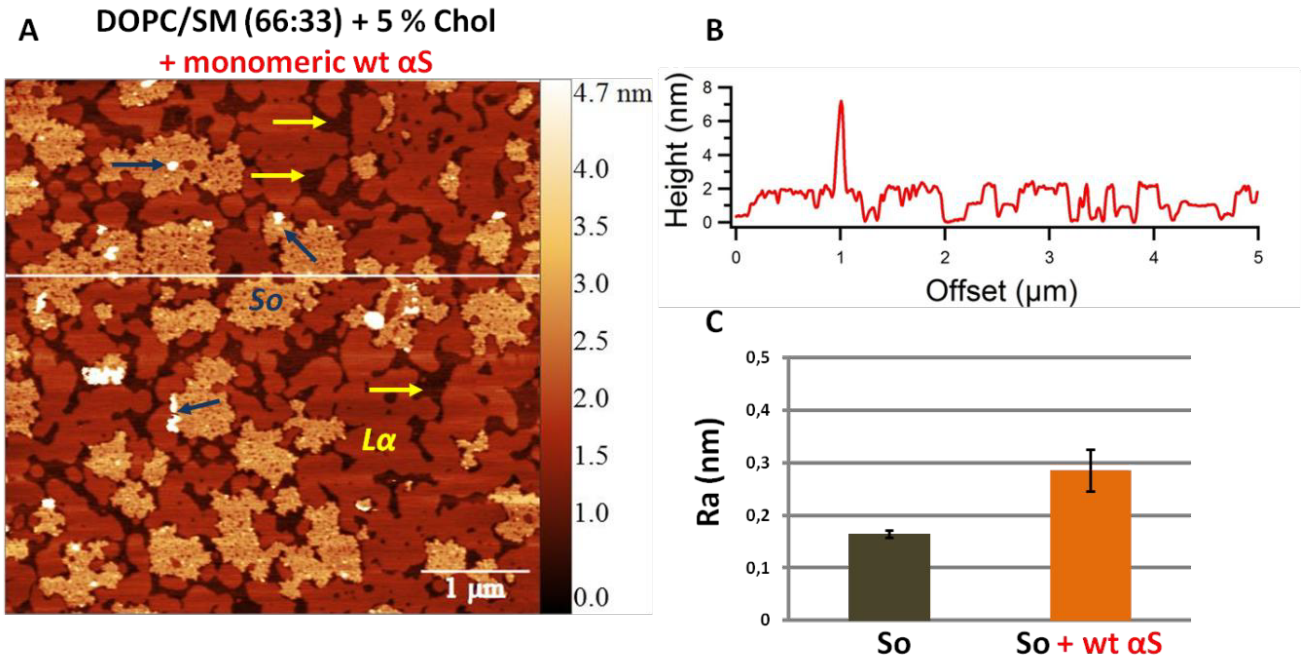

Membrane proteins: **Iron-mediated Alpha Synuclein (αS) aggregation**

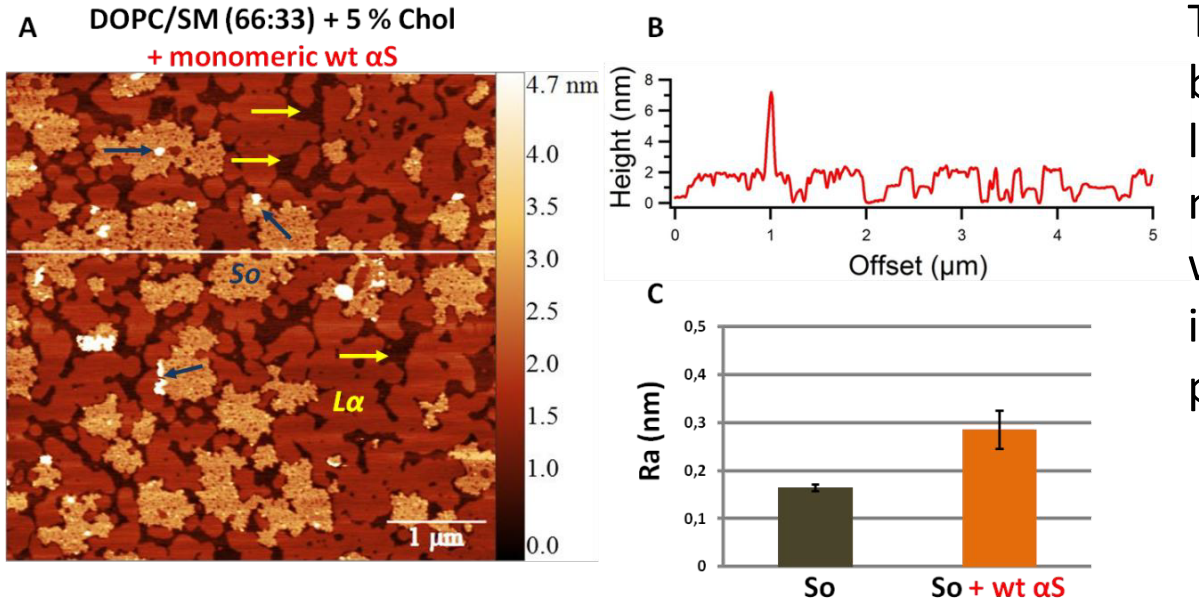

The wt αS seems to interact with both lipid phases (Lα and So) leading to a change in the morphology of raft-like domains which appear to have irregular and indented borders, as well as a more pronounced roughness.

A53T: mutant form of αS, responsible for an early stage familiar development of PD and more prone to aggregation
A53T seems to interact preferentially with the fluid lipid matrix causing damage sites without affecting the ordered domains

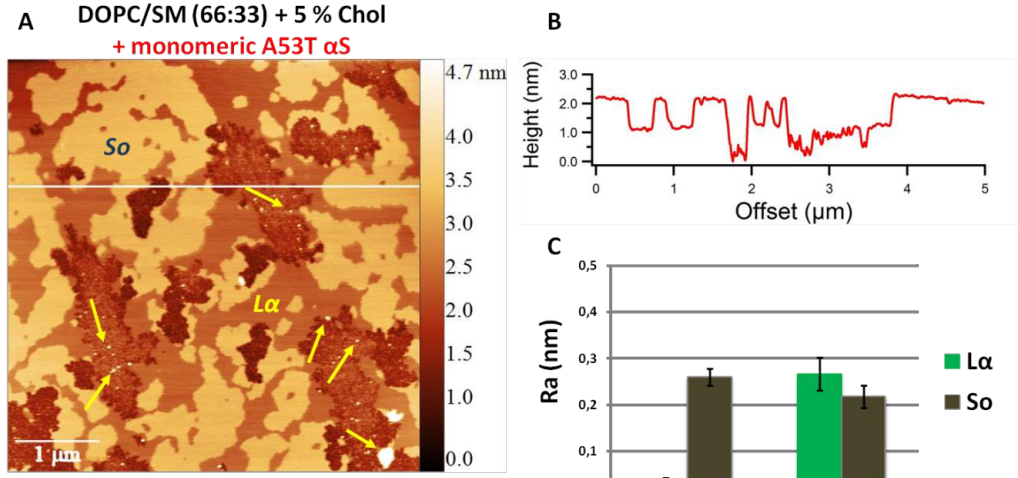

Lα	So	defect sites
29.3 %	32.2 %	38.5 %

Membrane proteins: **Iron-mediated Alpha Synuclein (αS) aggregation**

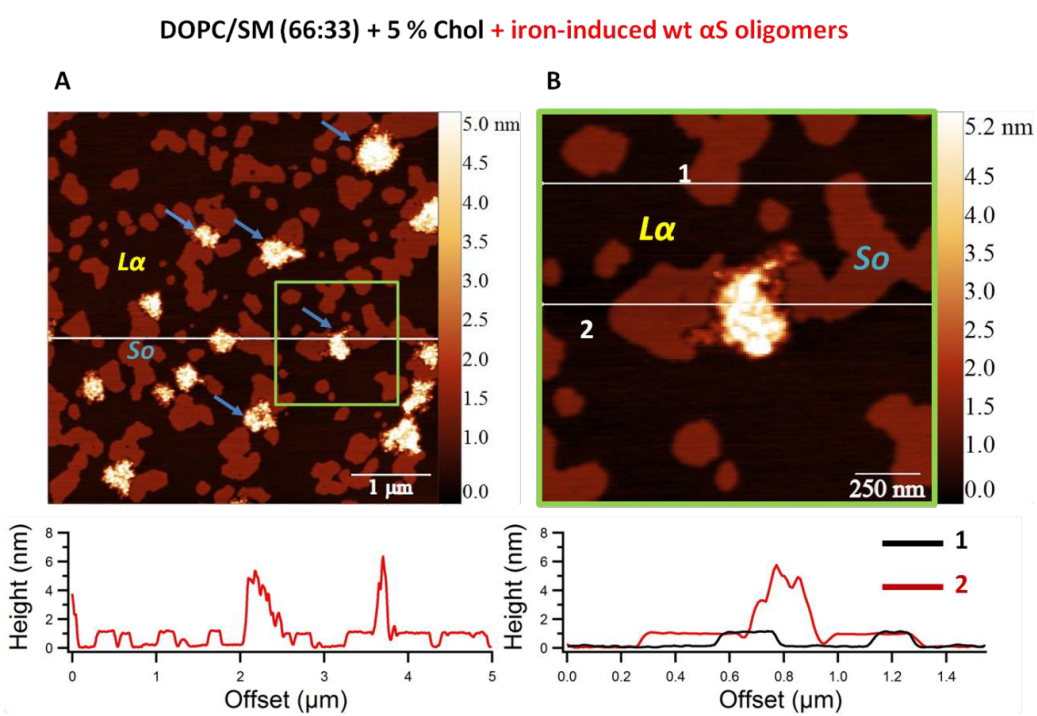

Iron-induced oligomers interaction with raft-like membranes revealed an accumulation of these misfolded structures on the ordered domains, forming protein clusters, for both wt and mutant A53T αS

The protein clusters of the mutant species are bigger in terms of dimensions and coverage of the membrane area, reflecting the faster rate of aggregation in the presence of iron compared to the wt αS

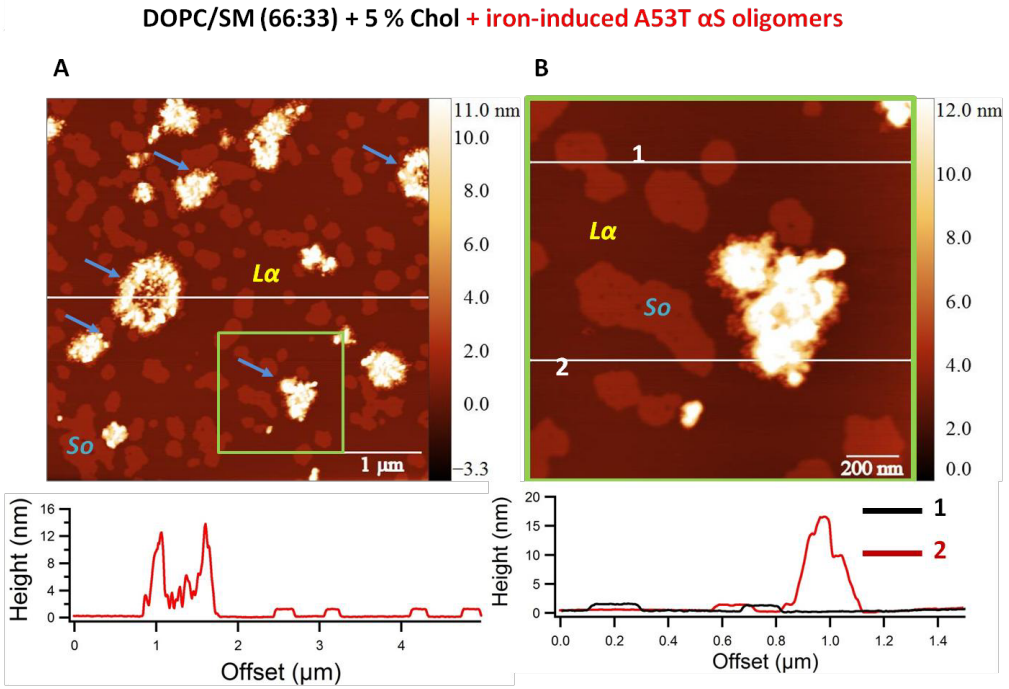

Purple membranes

The so-called **Purple Membranes (PM)** are part of the membrane of the archaea Halobacterium salinarium, an extremophile naturally found in salt saturated water.
This particular biological membrane **contains only one protein, bacteriorhodopsin (bR) and about seven different unusual membrane lipids** assembled in a hexagonal lattice of bR trimers (p3 crystallographic point group, 6.2 nm lattice constant).

The protein-lipid ratio has recently been determined to be **10 lipids per bR.**
The proteins represent 75% of PM mass and cover 50% of the membrane surface.
bR acts as a **light-driven vectorial proton pump** which converts photonic energy into a proton gradient across the membrane.
The induced electrochemical gradient is subsequently used by ATP-synthase as an alternative driving force to produce ATP in mediums particulary poor in oxygen.

The absorption spectrum of bR in its ground state (maximum absorbtion at 565 nm) is responsible for the purple colour of PM

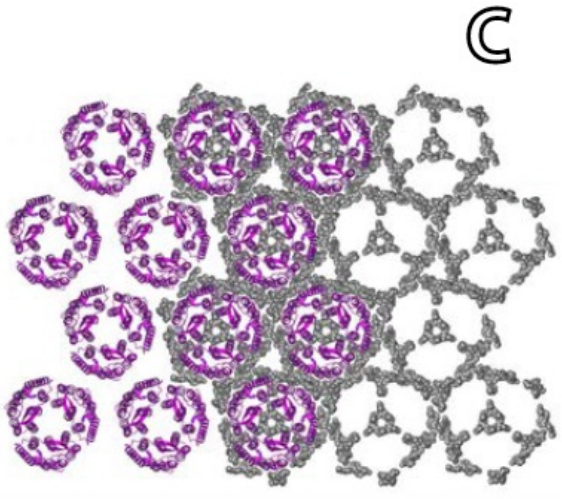

2D hexagonal lattice

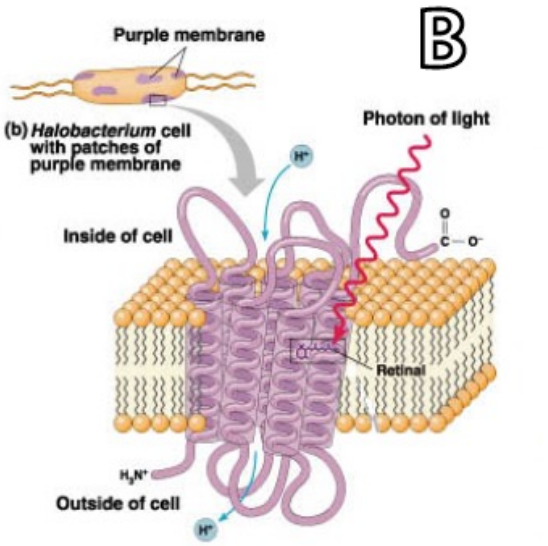

Purple membranes

PM is one of the best known biological membrane and an important model system to confront new theories and experimental methods.
bR was indeed the first integral membrane protein which structure was determined by X-ray crystallography of three-dimensional crystals grown in cubic lipid phase (non soluble proteins: difficulty in crystallization!)

N.B: membrane proteins are either peripheral (at the surface) and soluble in high ionic strenght acqueous solution (1 M salt) or integral, and can be solubilized only with detergent

All the protein membranes are coded by 20-30 % of the genome! But of all the known protein structures, only 5 % is of membrane proteins!

Purple membranes

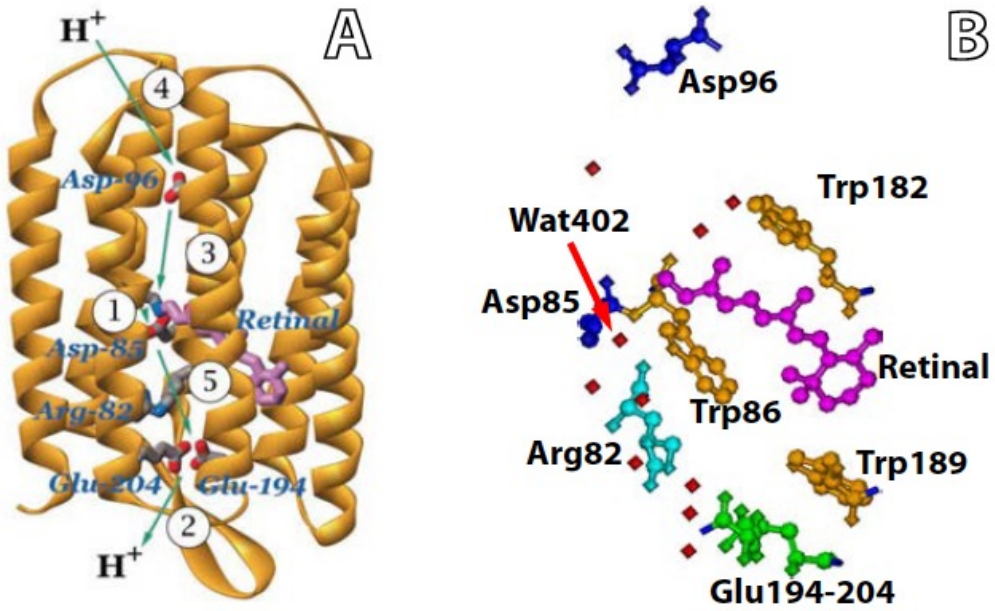

bR is an integral 26 KDa membrane protein composed 248 amino acids arranged in 7 transmembrane α-helices that surround a central cavity which encloses a chromophore, the retinal, linked to the protein backbone (Lys216 residue, helix G) via a Schiff base.

When the protein is in its fundamental/ground state (called bR state), the retinal chromophore adopts an all-trans configuration. Upon light absorption by the protein, the retinal can isomerize around its $C_{13} = C_{14}$ double bond, adopting a 13-cis configuration. This new chromophore conformation triggers a series of structural rearrangements in bR leading to the pumping of a proton from the inside to the outside of the archea.

Purple membranes

In PM, **bR molecules lateral and rotational movements are prevented by the crystalline assembly**. PM is rather rigid with a viscosity typically 10^3-10^4 higher than that of halobacterial membrane lipids.
Within one trimer, the proximity between the bR molecules allows direct protein-protein interactions through the formation of salt bridges, hydrogen bonds and van der Waals interactions between the α-helices of the different proteins involved.

These interactions are however not sufficient to explain the important trimer stability in which specific protein-lipid interactions are involved. The exceptional cohesion within a single trimer is believed to be related to the protein activity through cooperativity.

Purple membranes

PM contains many different lipids some of which are not found in any other membrane and are necessary for bR activity, also in reconstituted membranes. To date, seven different lipids have been reported :
three phospholipds, two glycolipids, squalene and traces of vitamin MK8.

The requirement of a fixed membrane composition indicates that **selective interactions occur between bR and certain lipid molecules** and that these interactions are essential for lattice assembly and bR function.

Phospholipids represent ~ 40% of PM lipids. their head-group comports two negative charges which makes them particularly hydrophilic. Fluorescence studies have demonstrated that phospholipids are located mainly in PM cytoplasmic leaflet inter-trimer space.
Glycolipids represent ~ 30% of PM lipids. Unlike phospholipids, glycolipids show clear patterns in PM diffraction experiments suggesting that they are specifically and tightly bound to bR.

HR-AFM in membrane biology

High-resolution AFM has been applied to the imaging of bacterial membrane proteins, deriving the free energy landscape for domains within single protein mole

AFM

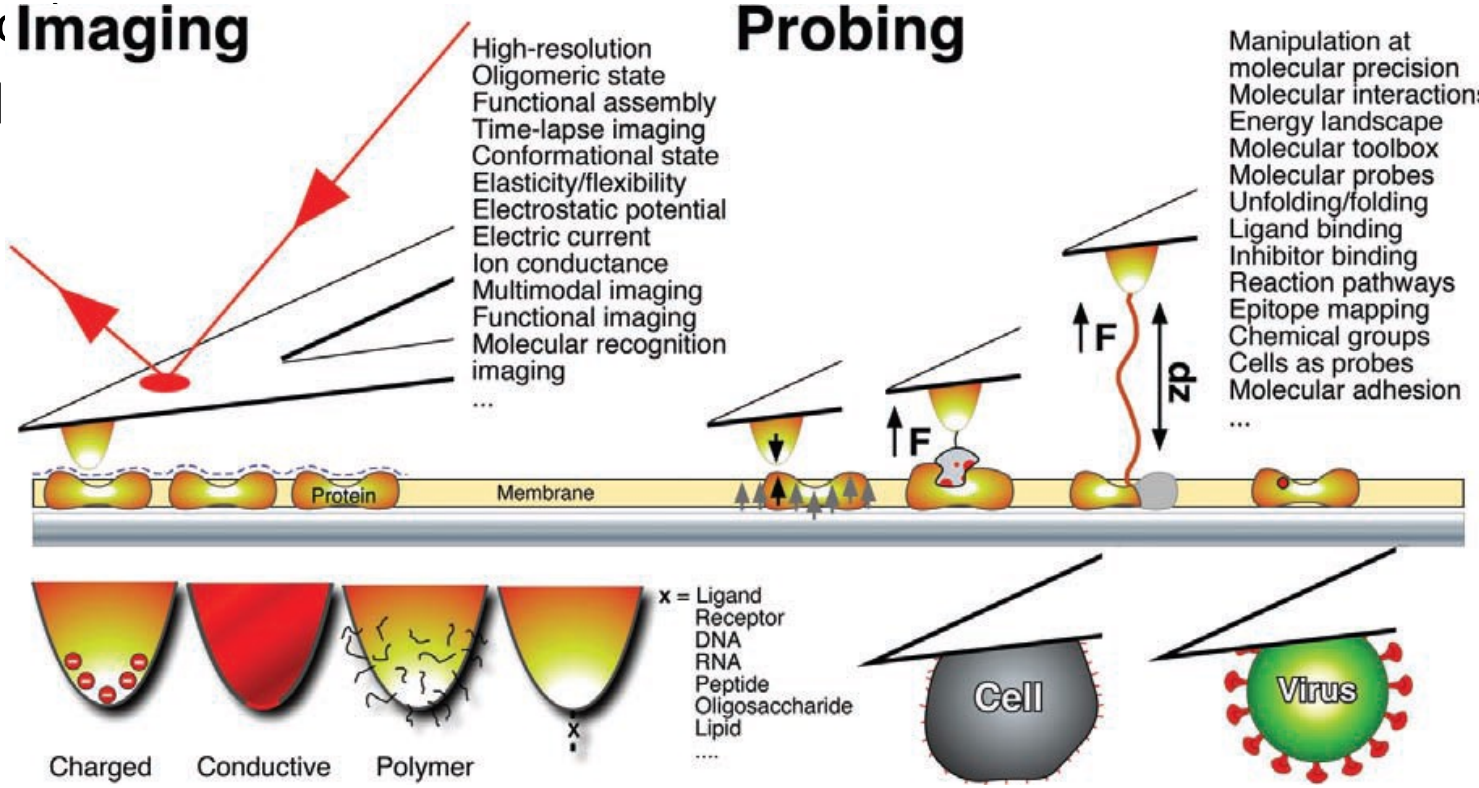

Imaging resolution in cell membranes: 10 nm
Imaging resolution in supported cell membranes: better than 1 nm (no fixing, labeling, Staining, room T, buffer solution)

S. Scheuring, D. Muller, H. Stalhberg, H.-A. Engel, A. Engel, *Eur. Biophys. J.* **31**, 172 (2002)

D.J. Muller et al. J. Mol. Biol. **(1999)** 285**, 1903-1909**

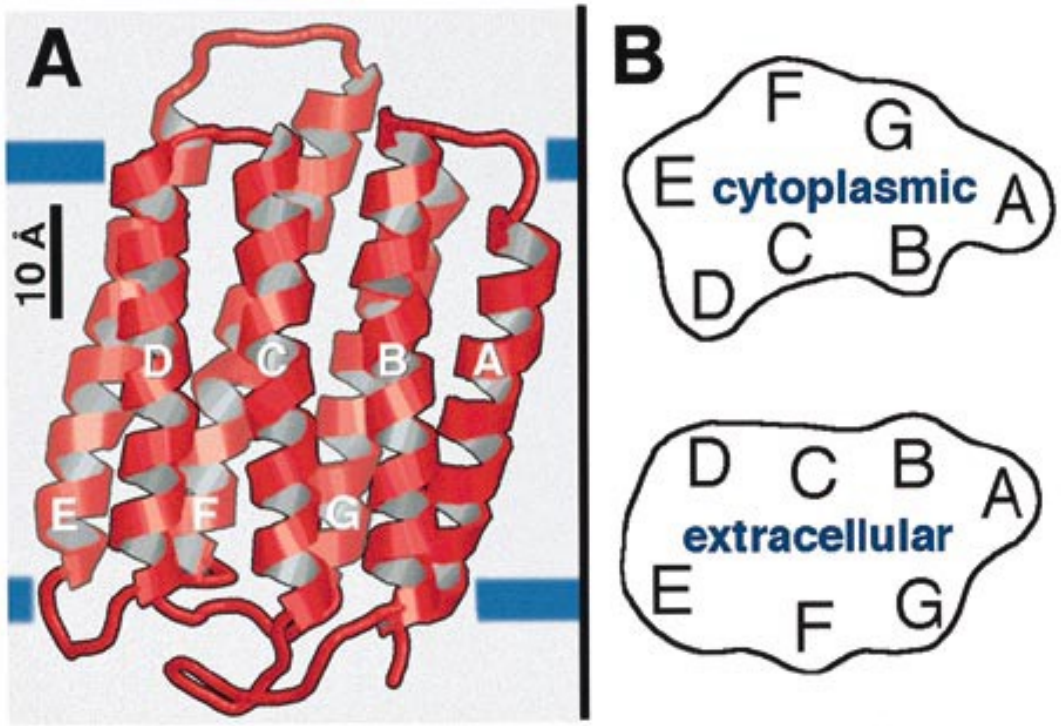

Structure of bacteriorhodopsin. (a) Ribbon representation as revealed by electron crystallography (Grigorieff et al., 1996). Because of their disordering, the N terminus of helix A and the C terminus of helix G were not resolved and the B-C loop was only partly resolved. Blue lines indicate the cytoplasmic and extracellular surfaces determined by Kimura et al. (1997).
(b) Outlines of 10 AÊ thick slices of the cytoplasmic and the extracellular BR surface.

D.J. Muller et al. / Biochimica et Biophysica Acta 1460 (2000) 27-38

PM reconstructed membrane on mica. Cytoplasmic vs. extracellular side

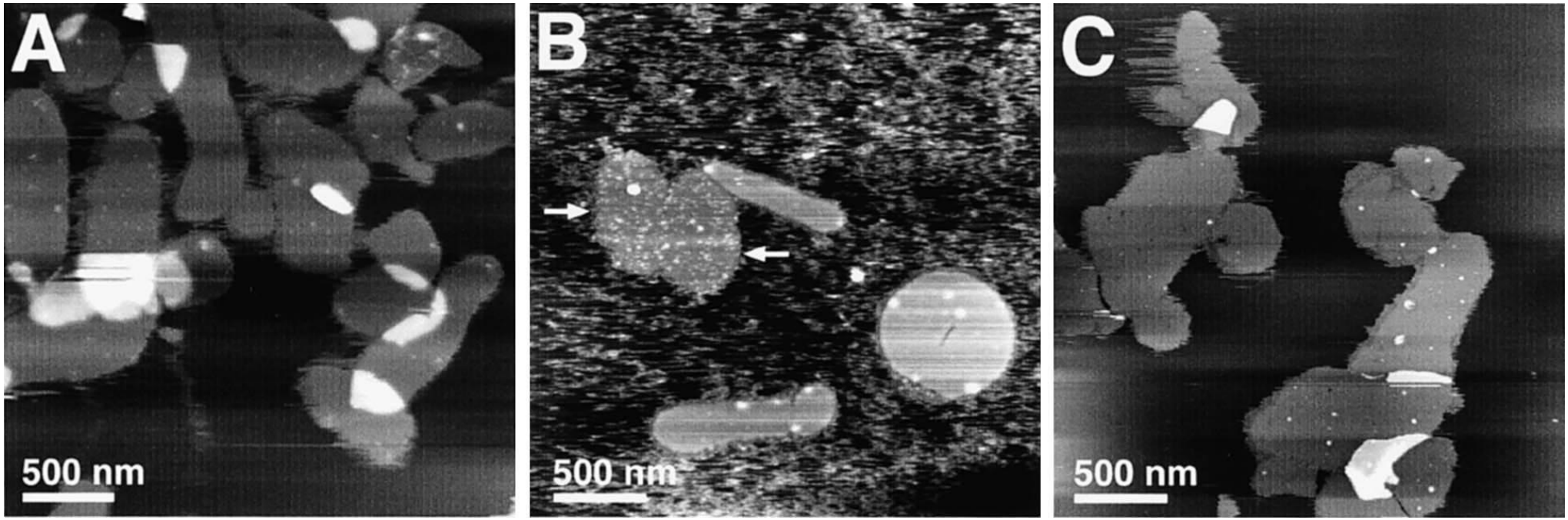

D.J. Muller et al. J. Mol. Biol. **(1999)** 285**, 1903-1909**

8.3(±1.9) Å **(**n . **398)**

6.4(±1.2) Å **(**n . **398)**

a=b=6.2±0.2 nm

The loops connecting the **alpha** -helices appeared to be disordered as they could not be resolved reliably.

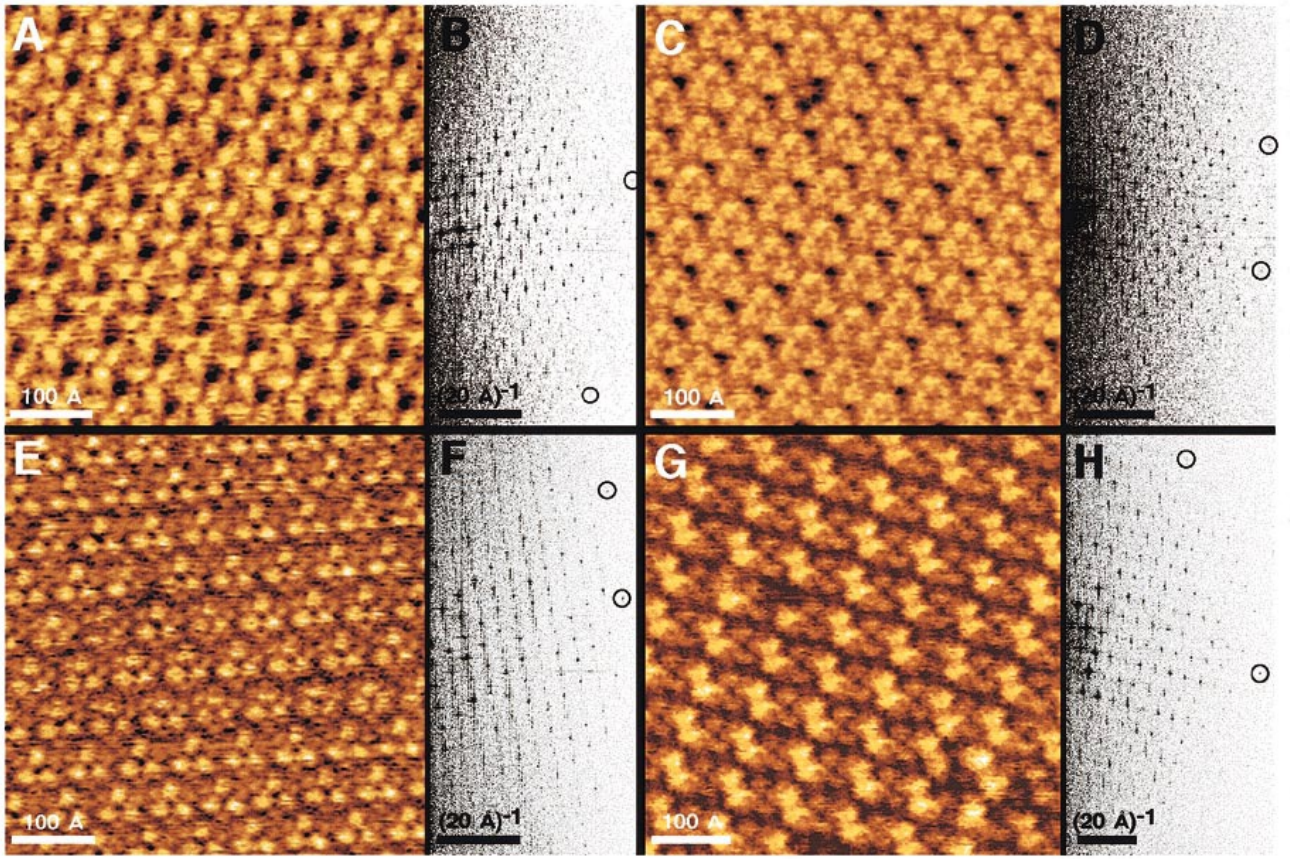

5.3(±0.7) Å **(**n . **320)**

in A protrusion arises from the loop connecting transmembrane **a** -helices E and F

(a) Native cytoplasmic surface recorded at 100 pN. (b) Power spectrum of (a). (c) Cytoplasmic surface recorded at 200 pN. (d). Power spectrum of (c). (e) Native extracellular surface recorded at 100 pN. (f) Power spectrum of (e). (g) Orthorhombic crystal of BR recorded at 100 pN. In this crystal form (p22121) the rows of BR dimers alternate, to expose either their cytoplasmic or their extracellular surfaces to the aqueous solution. (h) Power spectrum of (g).

N.B.: For the achievement of high resolution imaging a specific ionic concentration was required in order to balance van der Waals attractive forces with Electrostatic Double Layer repulsive forces (Muller & Engel 1997; Muller et al. 1999a).

D.J. Muller et al. J. Mol. Biol. **(1999)** 285**, 1903-1909 / Biochimica et Biophysica Acta 1460 (2000) 27-38**

Imaging of a statistically significant number of single proteins by AFM allows structural variability assessment and multivariate statistical classification to unravel the principal modes of the protein motion

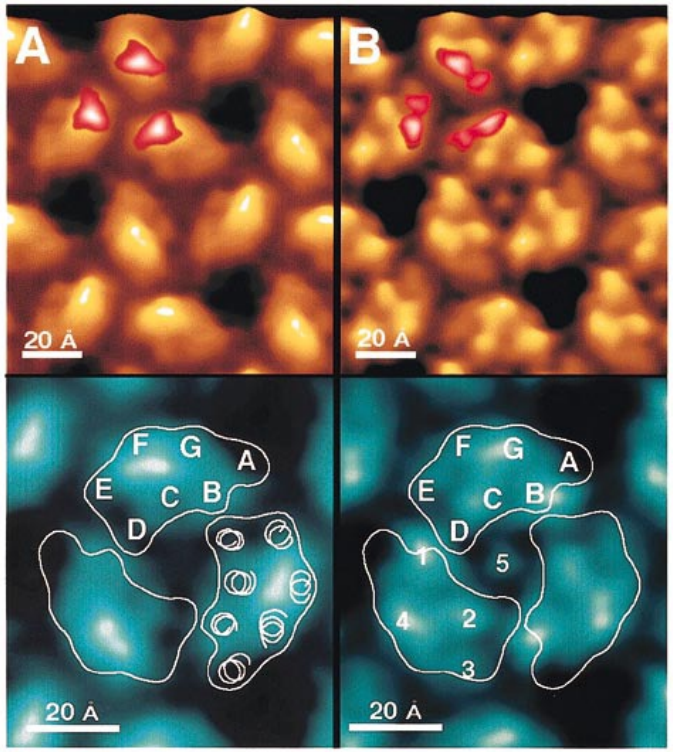

(C) Averaged extracellular surface of the bR trimer (average of 320 unit cells). The correlation average is displayed in perspective view (top, shaded in yellow brown) and in top view (bottom, in blue) with a vertical brightness range of 1 nm and exhibited a 6.1% root-mean-square (RMS) deviation from three-fold symmetry. To assess the flexibility of the different structures, standard deviation (S.D.) maps are calculated
(D) and had a range from 0.07 (lipid) to 0.12 nm (region of the FG loop).

D.J. Muller et al. J. Mol. Biol. **(1999)** 285**, 1903-1909**

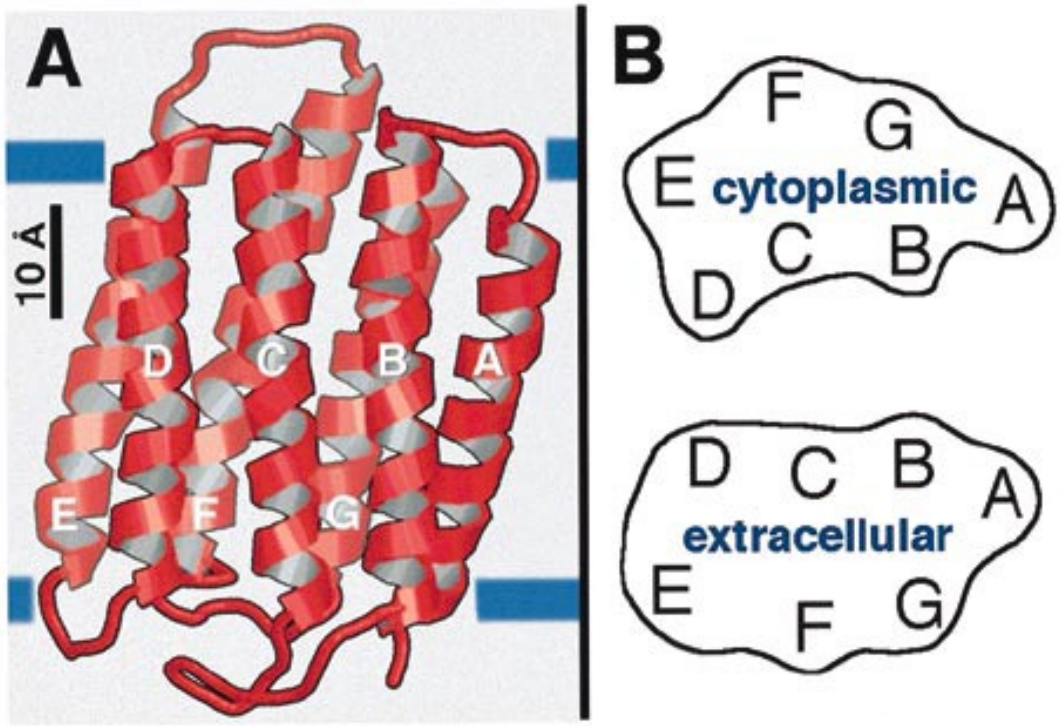

Structure of bacteriorhodopsin. (a) Ribbon representation as revealed by electron crystallography (Grigorieff et al., 1996). Because of their disordering, the N terminus of helix A and the C terminus of helix G were not resolved and the B-C loop was only partly resolved. Blue lines indicate the cytoplasmic and extracellular surfaces determined by Kimura et al. (1997).
(b) Outlines of 10 AÊ thick slices of the cytoplasmic and the extracellular BR surface.

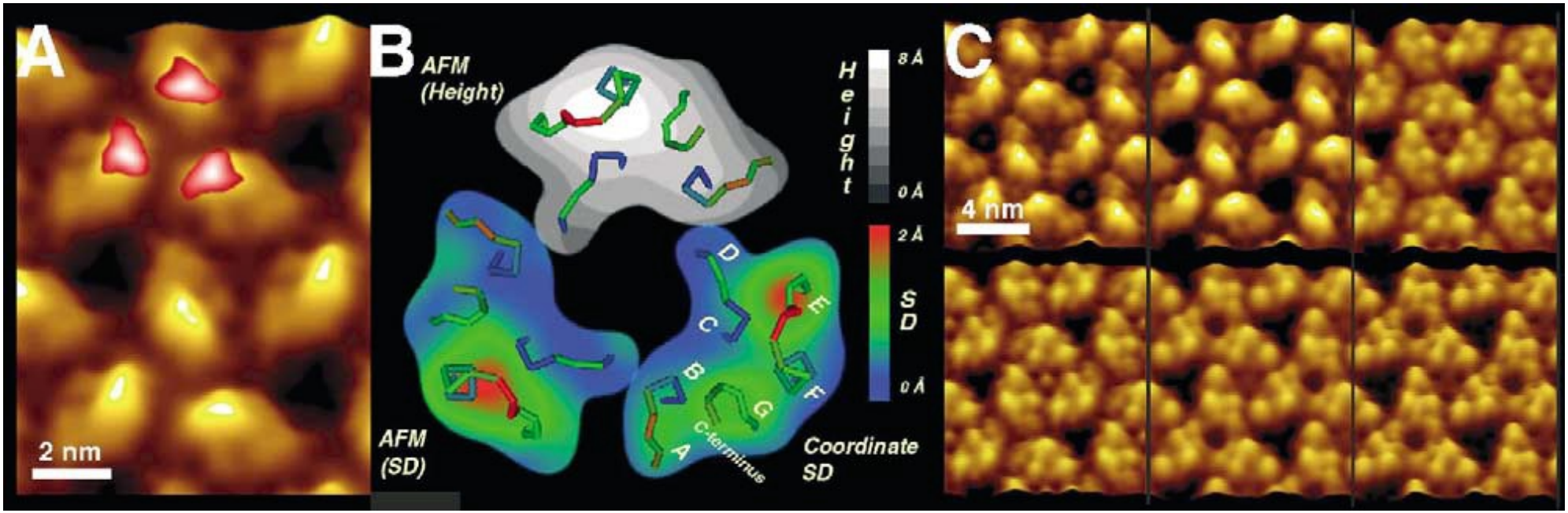

Fig. 16. Quantitative analysis of the native cytoplasmic purple membrane surface. (A) Correlation average of the AFM topograph recorded at an applied force of 100 pN (Müller et al., 1999b). Regions with enhanced flexibility are derived from SD maps and superimposed in red to white shades. (B) Different surface properties of bacteriorhodopsin. The surface loops are shown as backbone tracings colored according to the backbone coordinate root-mean-square deviation (SD) calculated after merging five different atomic models of bacteriorhodopsin (Heymann et al., 1999). The gray scale image shows the height map determined by AFM (A) with the prominent protrusion representing the EF loop. The colored monomers represent the SD between the atomic models, and of the height measured by AFM. (C) Unraveling the force induced structural changes of the cytoplasmic surface by multivariate statistical analysis. Top left: purple membrane imaged at 80 pN. Top center: same membrane imaged at approximately 100 pN. Top right: at about 150 pN the EF loop is bent away while the shorter polypeptide loops of the cytoplasmic surface become visible. Bottom row: three conformations differing in their central protrusion are observed at approximately 180 pN. Topographs exhibit a vertical range of 1 nm and are displayed as relief tilted by 5°.

Dynamics of bR on purple membranes

Ando's group, Angew Chem Int Ed, 2011

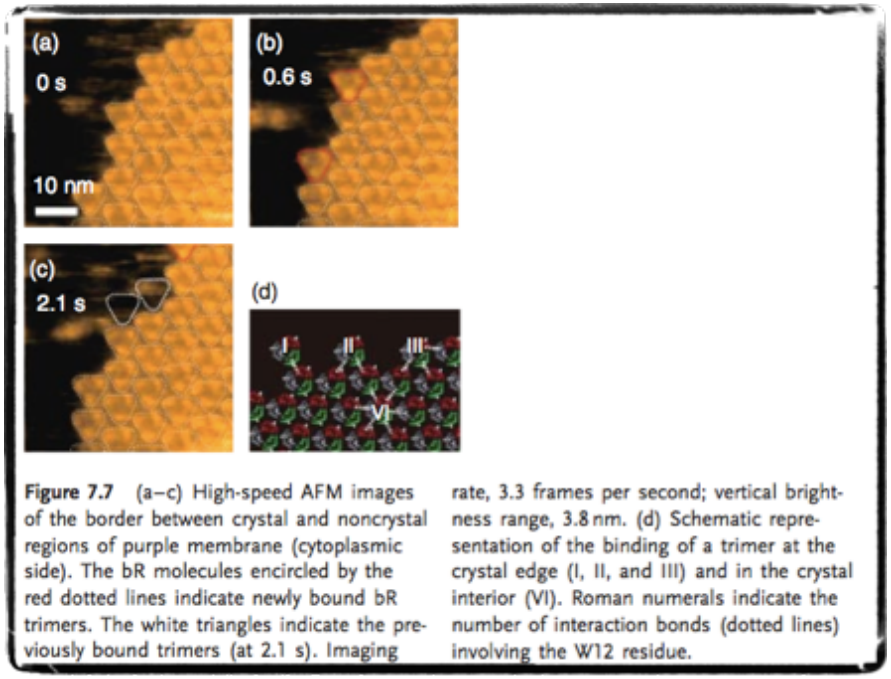

Figure 7.7 (a–c) High-speed AFM images of the border between crystal and noncrystal regions of purple membrane (cytoplasmic side). The bR molecules encircled by the red dotted lines indicate newly bound bR trimers. The white triangles indicate the previously bound trimers (at 2.1 s). Imaging rate, 3.3 frames per second; vertical brightness range, 3.8 nm. (d) Schematic representation of the binding of a trimer at the crystal edge (I, II, and III) and in the crystal interior (VI). Roman numerals indicate the number of interaction bonds (dotted lines) involving the W12 residue.

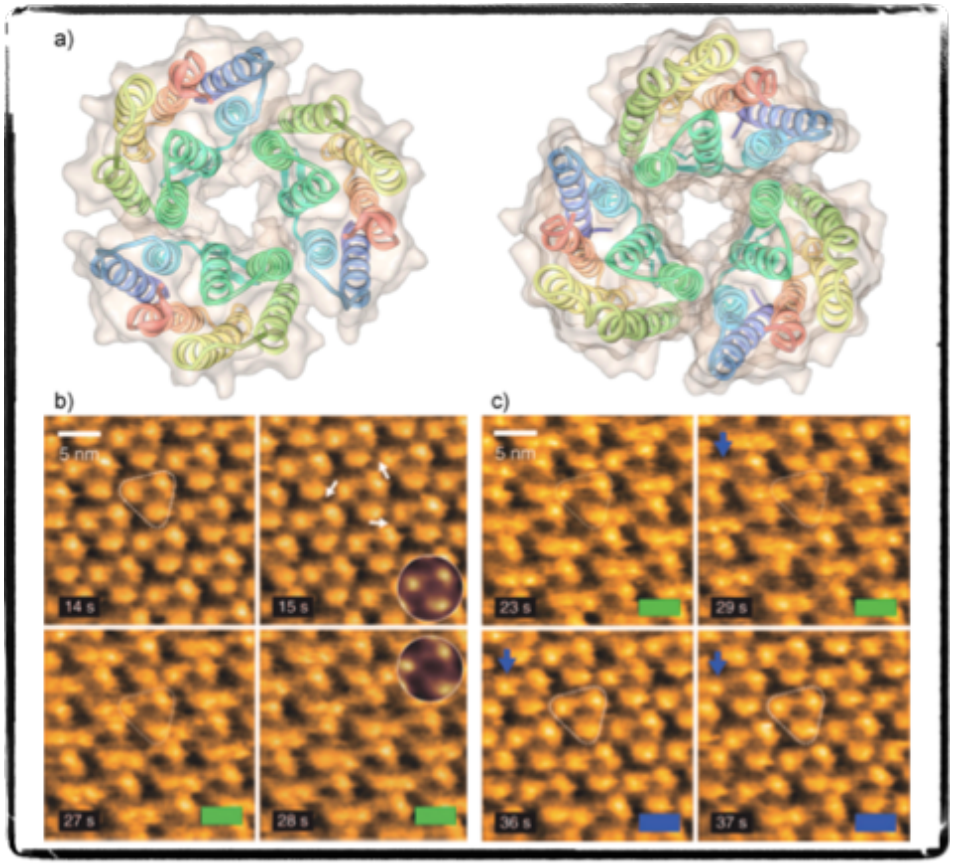

bR molecules with two binding partners associated for longer time periods to the array than proteins that had only one neighbor. Statistical assessment of the dissociation frequencies allowed the calculation of the **strength of a single bR–bR interaction of 1.5kBT (0.9 kcal/mol), resulting in a stability of about 5.4 kcal/ mol for the purple membrane arrays**, in good agreement with ensemble measurements by calorimetry

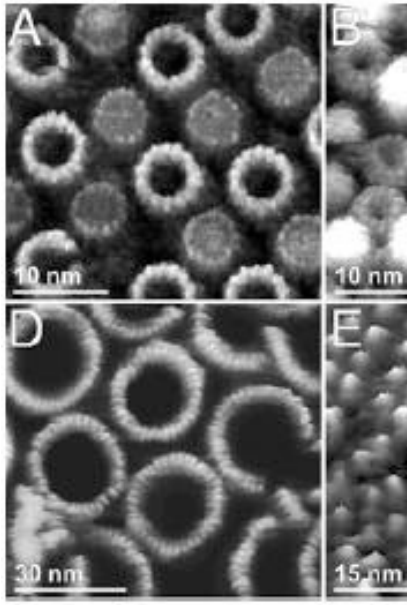

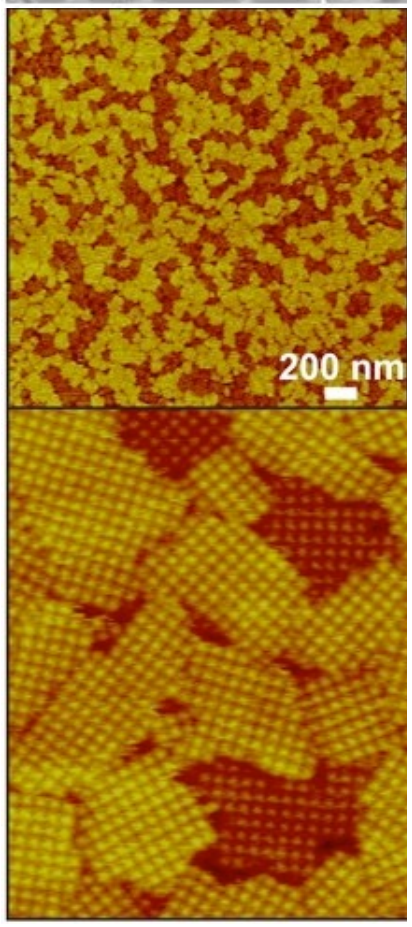

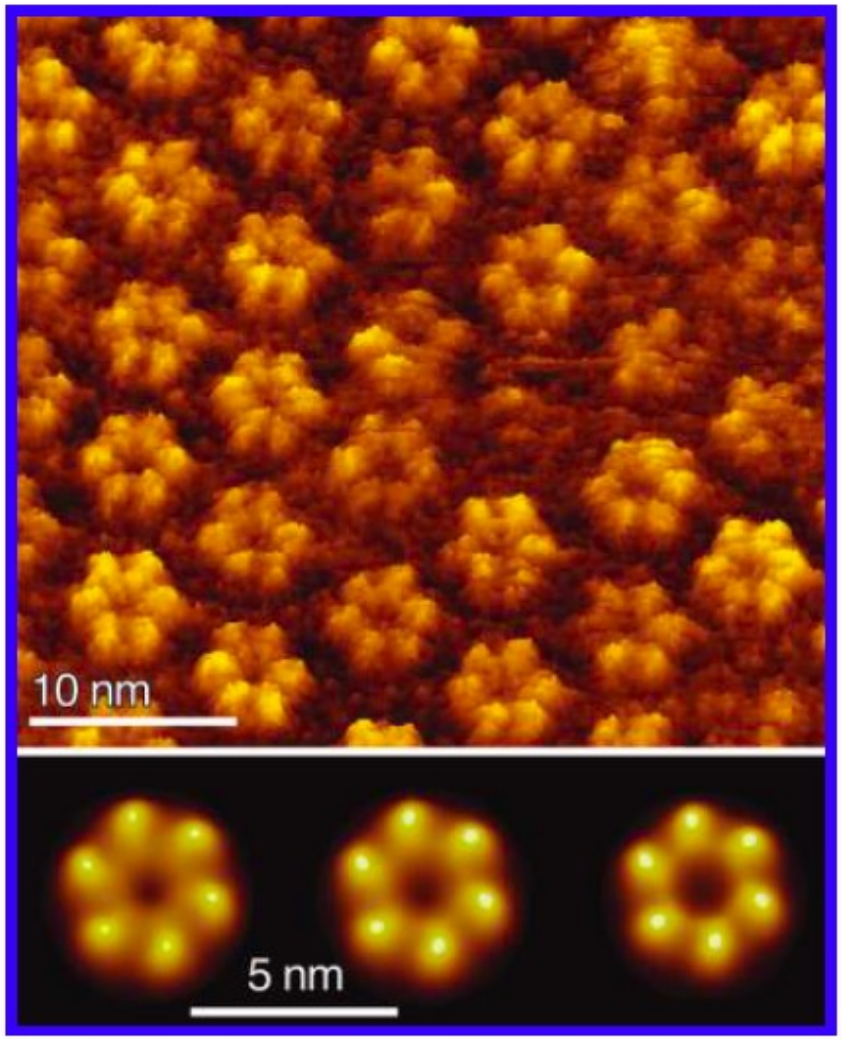

FIGURE 4: Watching communication channels at work. High-resolution AFM topograph showing the extracellular surface of Cx26 gap junction hemichannels. The gap junction membranes have been dissected with the AFM probe to expose their extracellular surface (*27*). The bottom row shows the conformational change of hemichannels in response to Ca^{2+}. The closed channels (left) switch, via an intermediate conformation (middle), to the open state (right) in the presence of 0.5 mM Ca^{2+}. Hemichannels in the bottom row represent correlation averages.

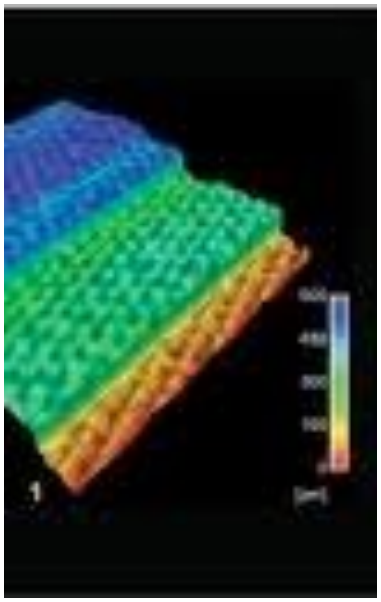

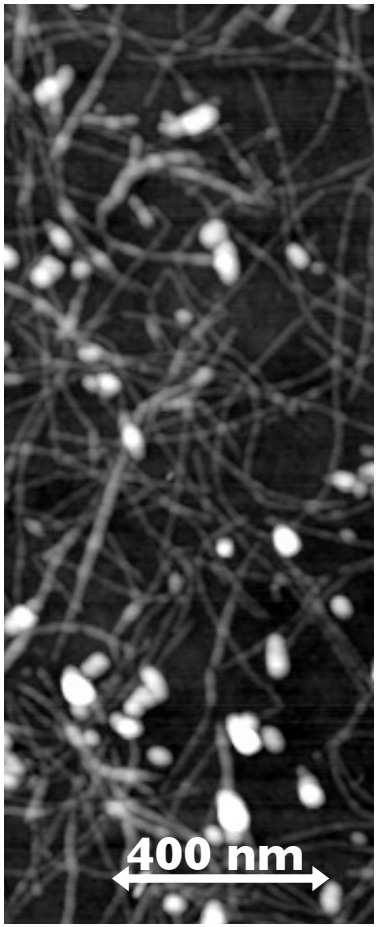

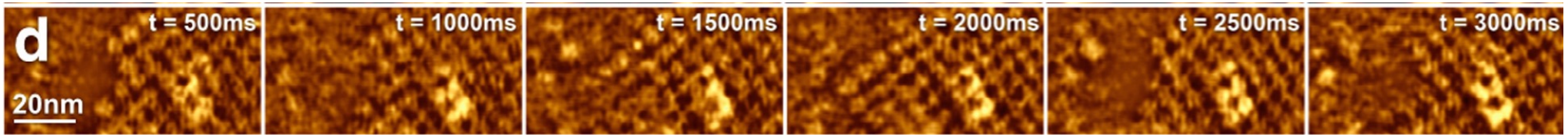

Using HS-AFM in contact mode, applying additional force s the junctional microdomains were dissected, revealing that the adhesion function of the proteins was cooperative: the entire membrane patches dissociated at once. From high spatial and temporal res. Assembly/dissasembly of auqaporin-0 and connexons to/from functional microdomains, with interaction strenght of -2.7 K_BT

HS-AFM on life cell

2.7 s/frame, with bright-field illumination

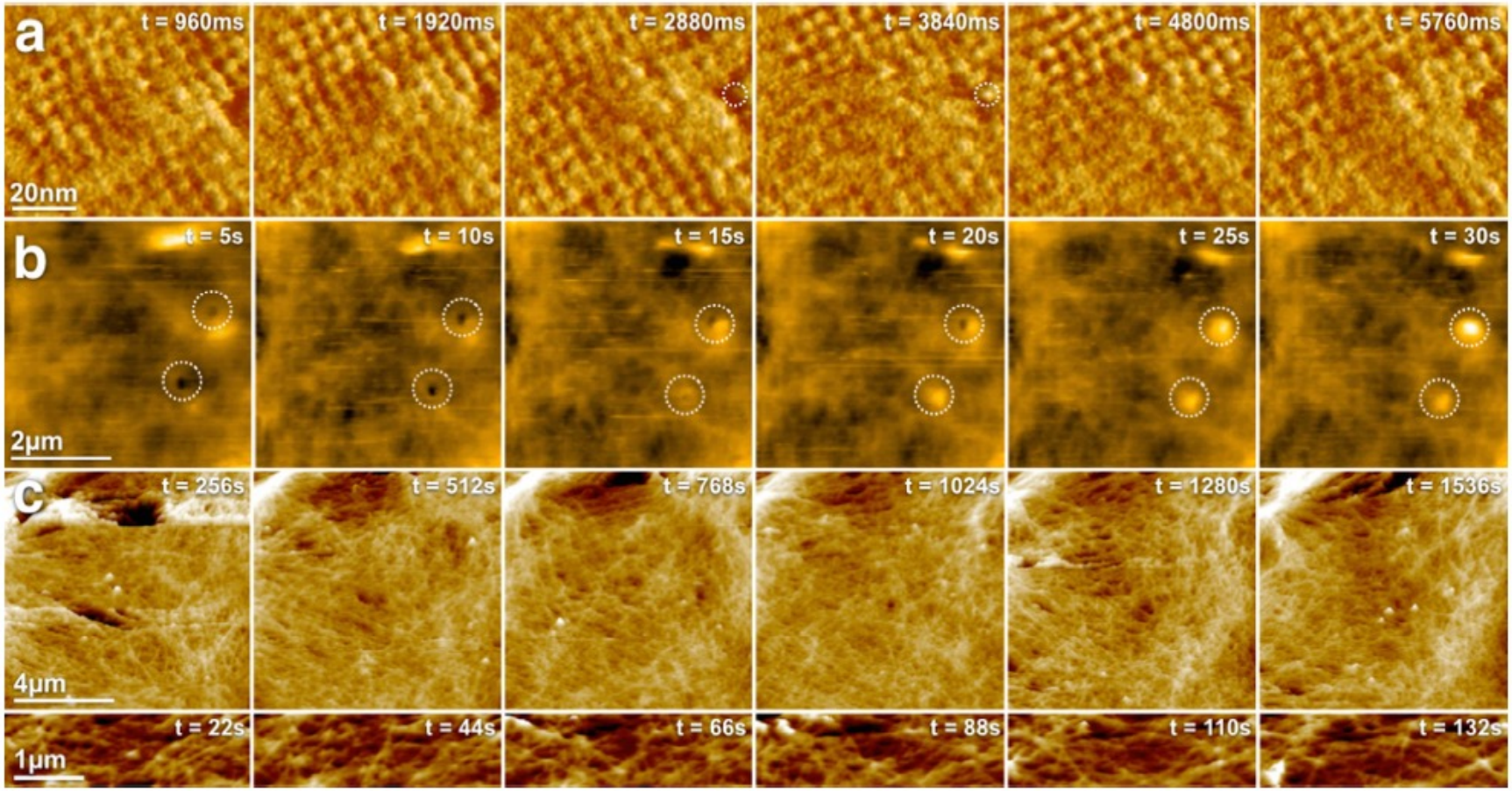

Fig. 2. HS-AFM applications on life cells. (a) High-resolution HS-AFM imaging of AQP0 in junctional microdomains in native eye lens cells. The dynamic association of individual AQP0 could be observed (outline). (b) Endocytosis events observed by HS-AFM on HeLa cells. (c) Dynamic PeakForce tapping imaging of the membrane cortex underneath the plasma membrane of 3T3 fibrobl

Colom, A., Casuso, I., Rico, F. and Scheuring, S. (2013) A hybrid high-speed atomic force–optical microscope for visualizing single membrane proteins on eukaryotic cells. Nat. Commun. 4.

Figure 5

Atomic force microscopy (AFM) images of the $\alpha_3\,\beta_3$ subcomplex at the C-terminal surface. (*a*) Schematic for F_1-ATPase. (*b*) Averaged AFM image obtained in nucleotide-free condition. (*c*) The C-terminal surface of crystal structure of a nucleotide-free $\alpha_3\,\beta_3$ subcomplex. (*d*) Simulated AFM image of panel *c*. (*e*) Averaged AFM image obtained in 1-mM AMP-PNP. (*f*) The C-terminal surface of crystal structure of an $\alpha_3\,\beta_3$ subcomplex obtained in ATP. (*g*) Simulated AFM image of panel *f*. (*h*) Successive AFM images showing counterclockwise rotary propagation of conformational change of an $\alpha_3\,\beta_3$ subcomplex at the C-terminal surface captured by high-speed AFM in the presence of 2 μM ATP, at 12.5 fps. The red circle marks the highest pixel position in each image. The color scale placed at the right-hand side of panels *b* and *f* indicate the *z*-scale for the respective images. Adapted with permission from Reference 99.

High-Speed AFM and Applications to Biomolecular Systems

Toshio Ando,[1,2] Takayuki Uchiashi,[1,2] and Noriyuki Kodera[2]

The $\alpha_3\beta_3\gamma$ subcomplex of F_1-ATPase (a part of ATP synthase) is the minimum complex for the full ATPase activity. About half the length of the long γ subunit is inserted into the central cavity formed by a ring-shaped $\alpha_3\beta_3$ where three α subunits and three β subunits are arranged alternately (1). Three ATP binding sites locate at the α-β interfaces, mainly in the β subunits. The $\alpha_3\beta_3\gamma$ subcomplex is a rotary motor (34, 48, 68, 115) (**Figure 5*a***). The γ subunit rotates in the stator $\alpha_3\beta_3$ ring driven by rotary hydrolysis of ATP at the three β subunits. The rotation occurs in the counterclockwise direction as viewed from the exposed side of the γ subunit (or from C-terminal side of $\alpha_3\beta_3$). In the ATPase cycle, three β subunits take different chemical states: ATP-bound, ADP-bound, and nucleotide-free (empty) states (1, 34). Each chemical state cyclically propagates over the three β subunits. Thus, there is strong cooperativity between β subunits.

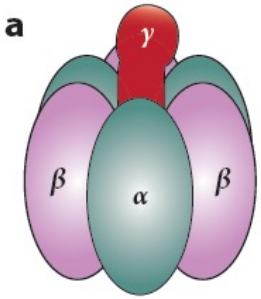

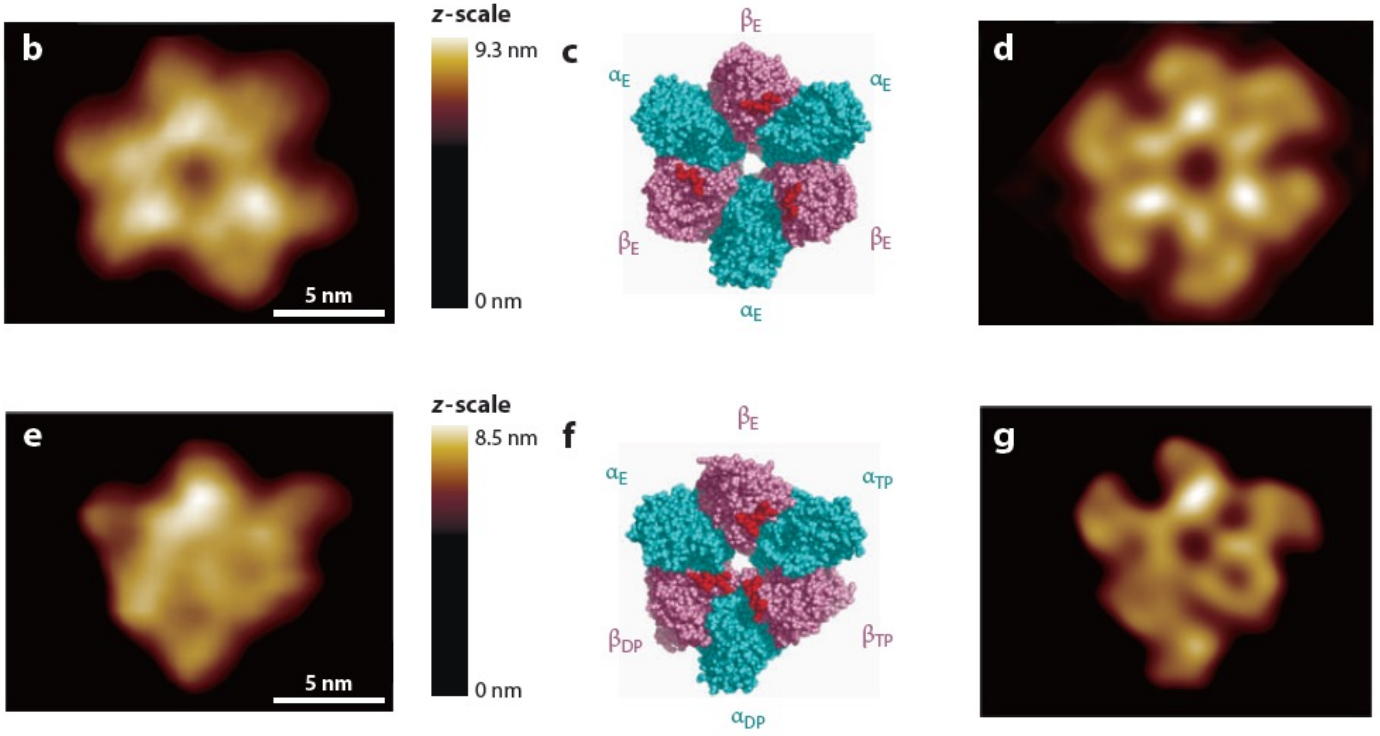

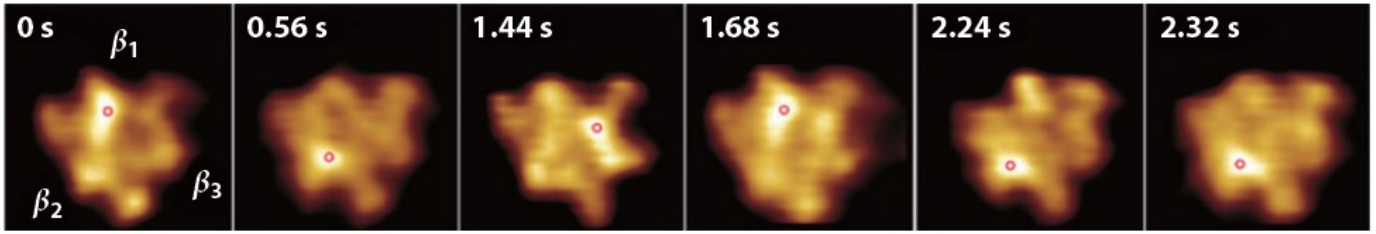

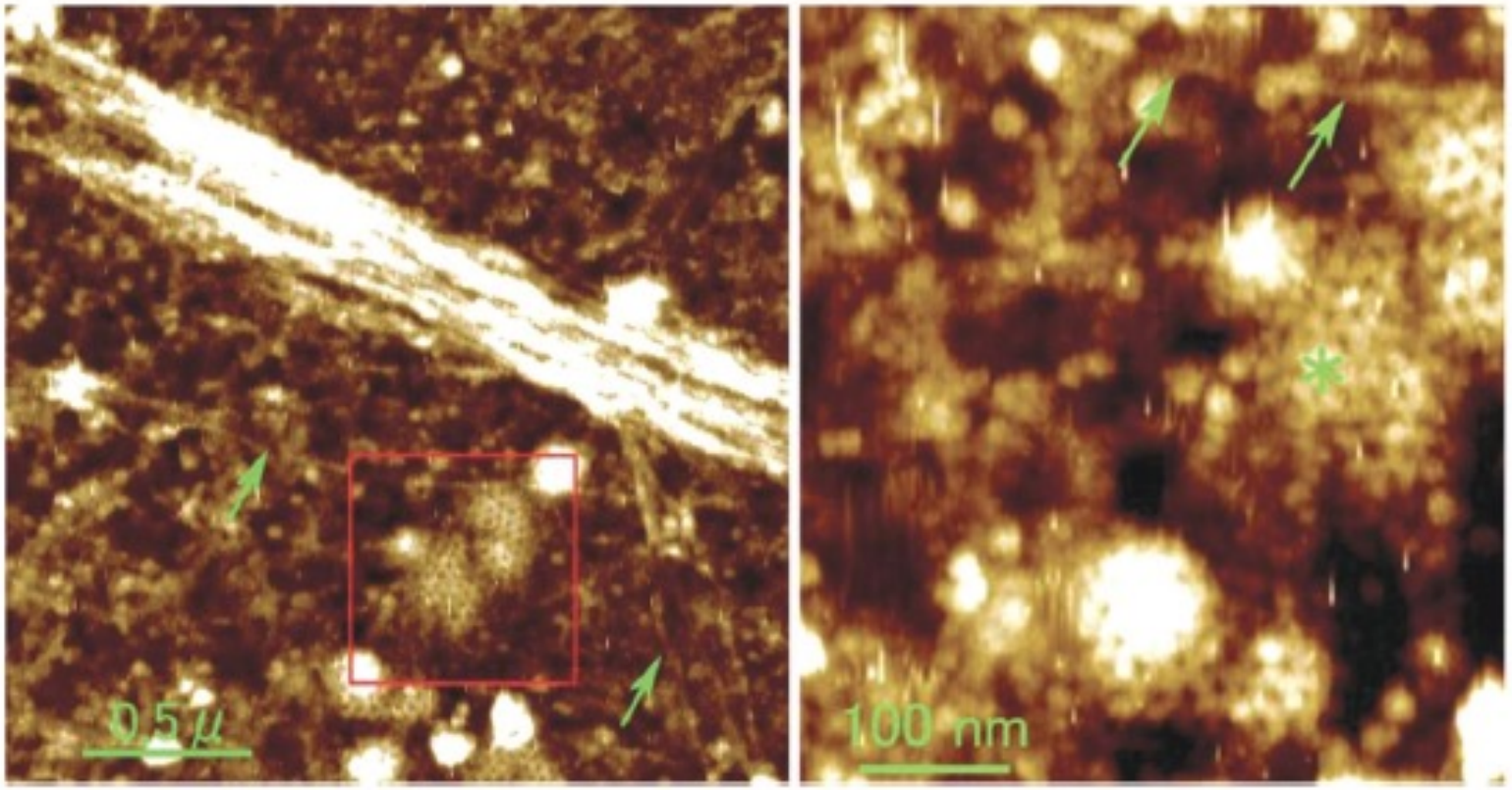

Fig. 18 AFM image of clathrin coats and actin filaments at the cytoplasmic surface of the plasma membrane. The right figure shows an enlarged view of the boxed area in the left figure. Clathrin-coated pits are clearly observed in the boxed area. Arrows indicate actin filaments. From ref. 95, Figure 6 with permission.

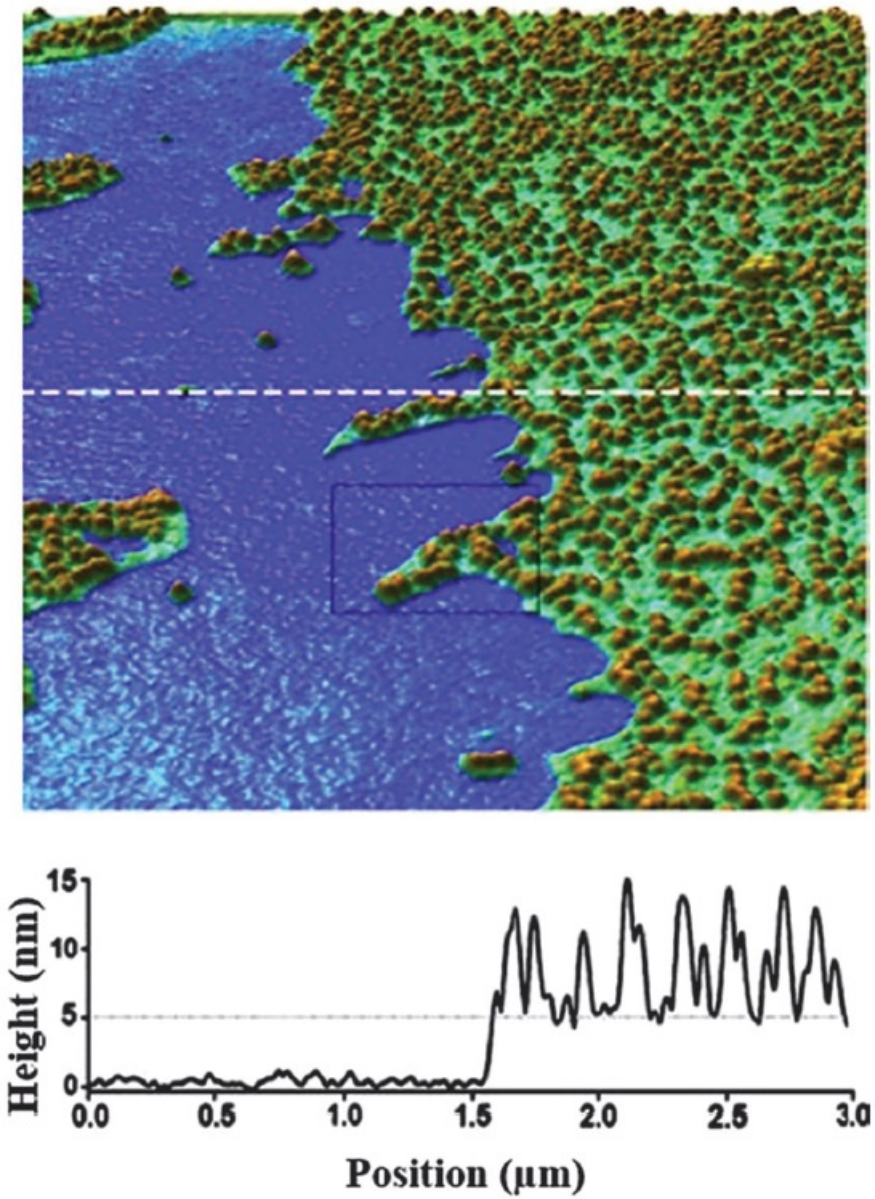

Fig. 17 AFM image of South African frog oocyte membranes (cytosolic side). Poly-L-lysine-coated glass (blue), the lipid bilayer membrane (turquoise), and the membrane proteins (brown). The height profile along the broken line is presented at the bottom. From ref. 91, Figure 6 with permission.

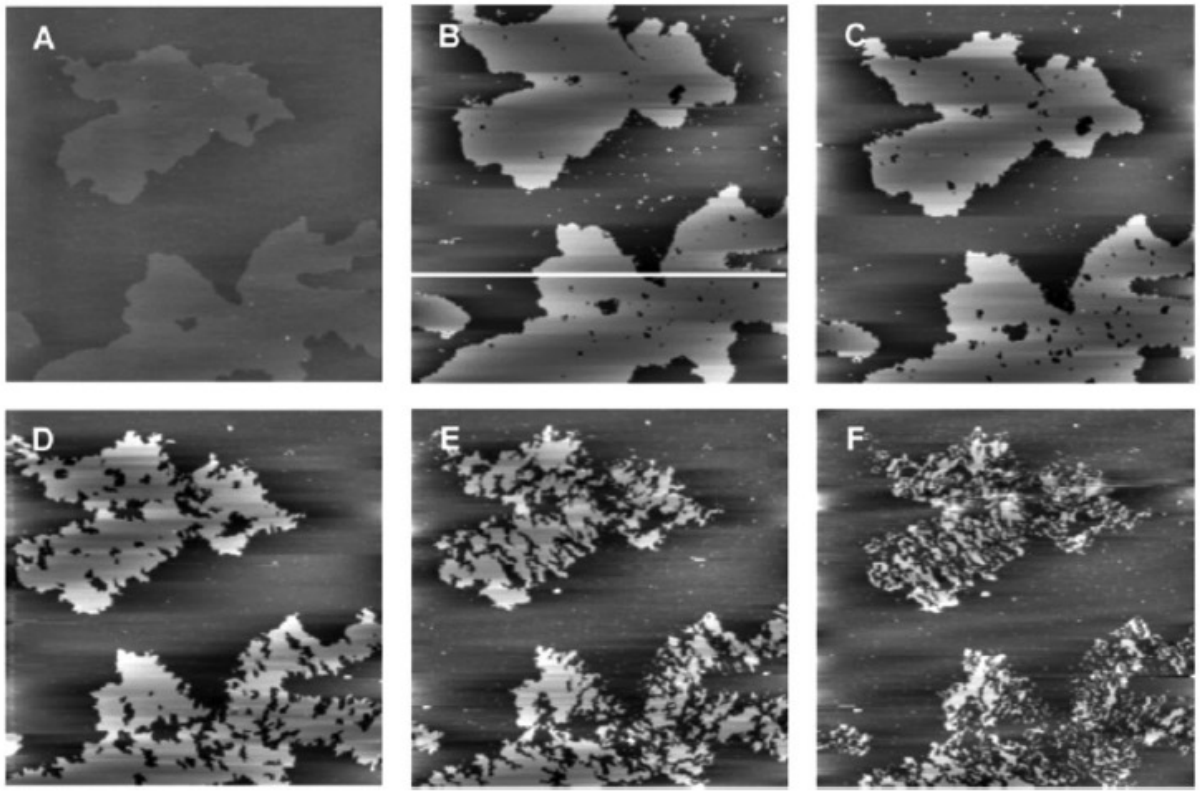

Fig. 14 Supported lipid membranes treated with TX-100. (A) An AFM height image (20 × 20 μm^2) of a mixed DOPC/DPPC bilayer prior to TX-100 addition. (B–F) Serial images after the addition of 0.48 mM TX-100 for 3.5 min (B), 10 min (C), 30 min (D), 60 min (E), and 90 min (F). Adapted from ref. 108, Figures 2A–F with permission.

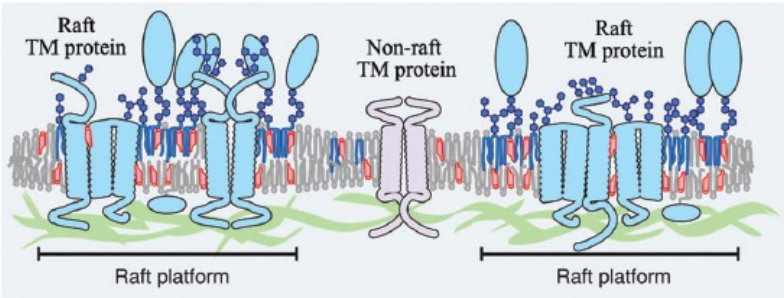

Fig. 3 Lipid raft domains in cell membranes. Adapted from ref. 25, Figure 2b with permission.

Self-organized monolayers (on liquid surfaces)

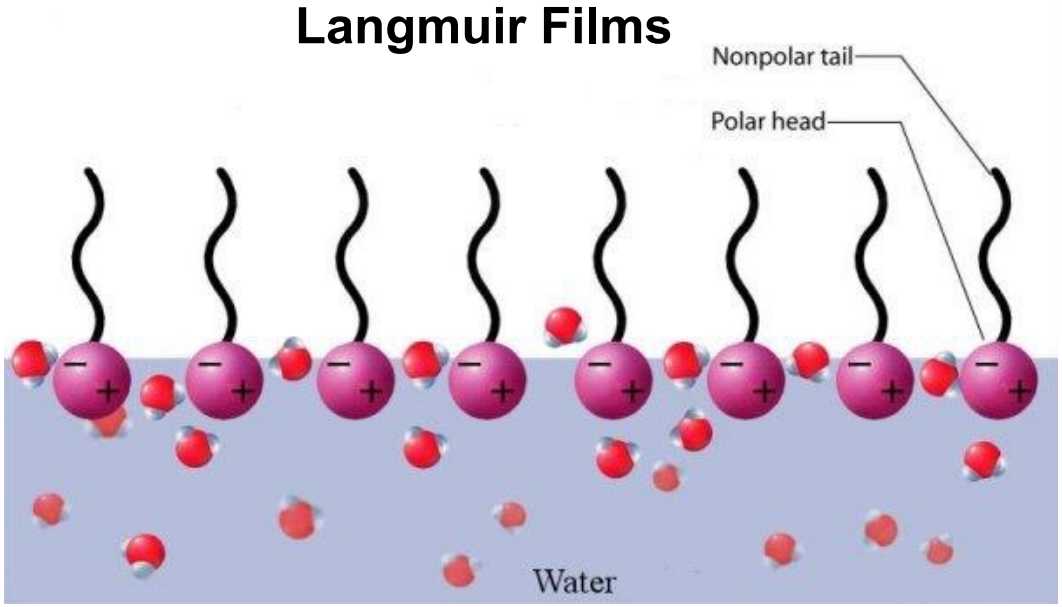

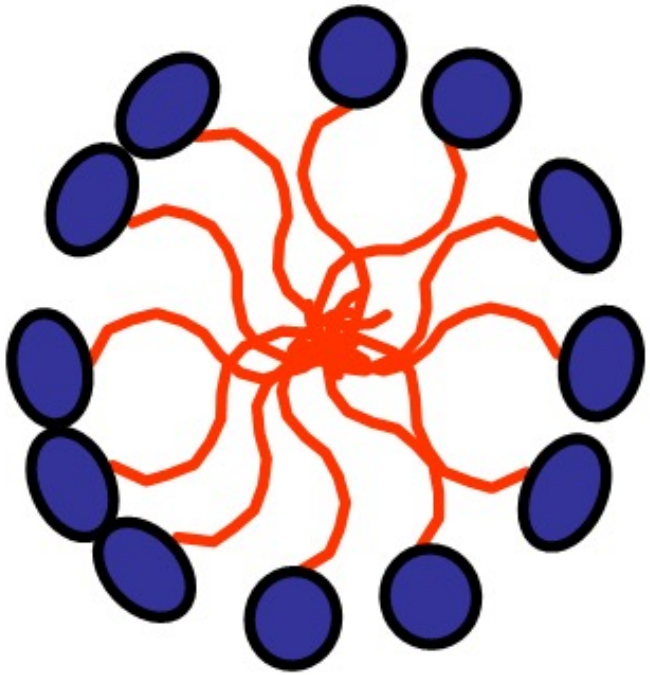

The term “molecular self-assembly” refers to spontaneous formation of an ordered molecular overlayer on the surface, often proceeding through several consecutive stages where 1D and 2D ordered structures can also exist.

Thermodynamically, molecular self-assembly proceeds toward the state of lower entropy , and must therefore be compensated by the establishment of intermolecular and molecule-surface interactions.

Self-organized monolayers (on liquid surfaces)

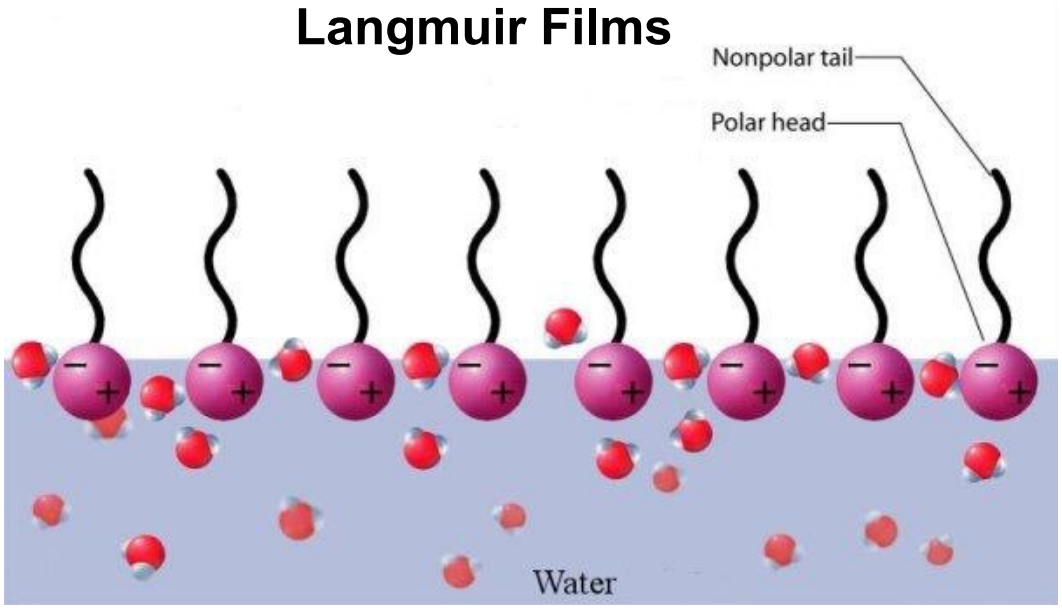

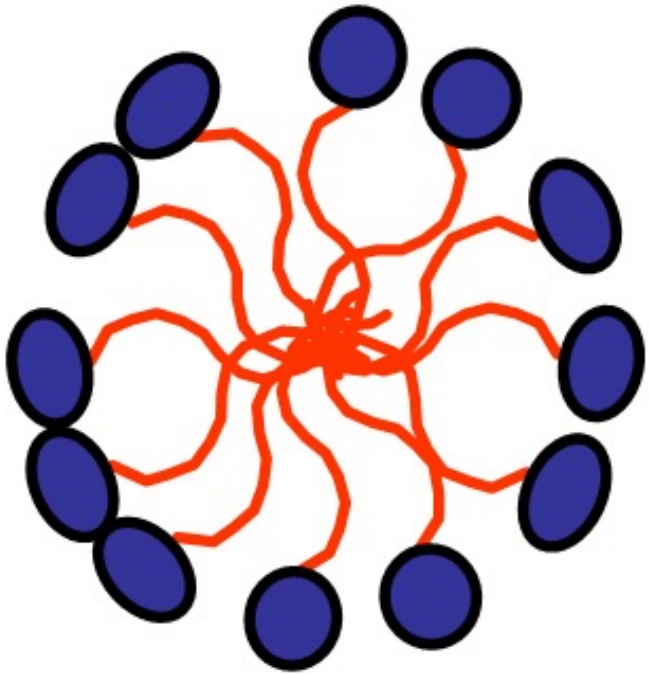

The term “molecular self-assembly” refers to spontaneous formation of an ordered molecular overlayer on the surface, often proceeding through several consecutive stages where 1D and 2D ordered structures can also exist.

Thermodynamically, molecular self-assembly proceeds toward the state of lower entropy , and must therefore be compensated by the establishment of intermolecular and molecule-surface interactions.

Self-organized monolayers (on solid surfaces)

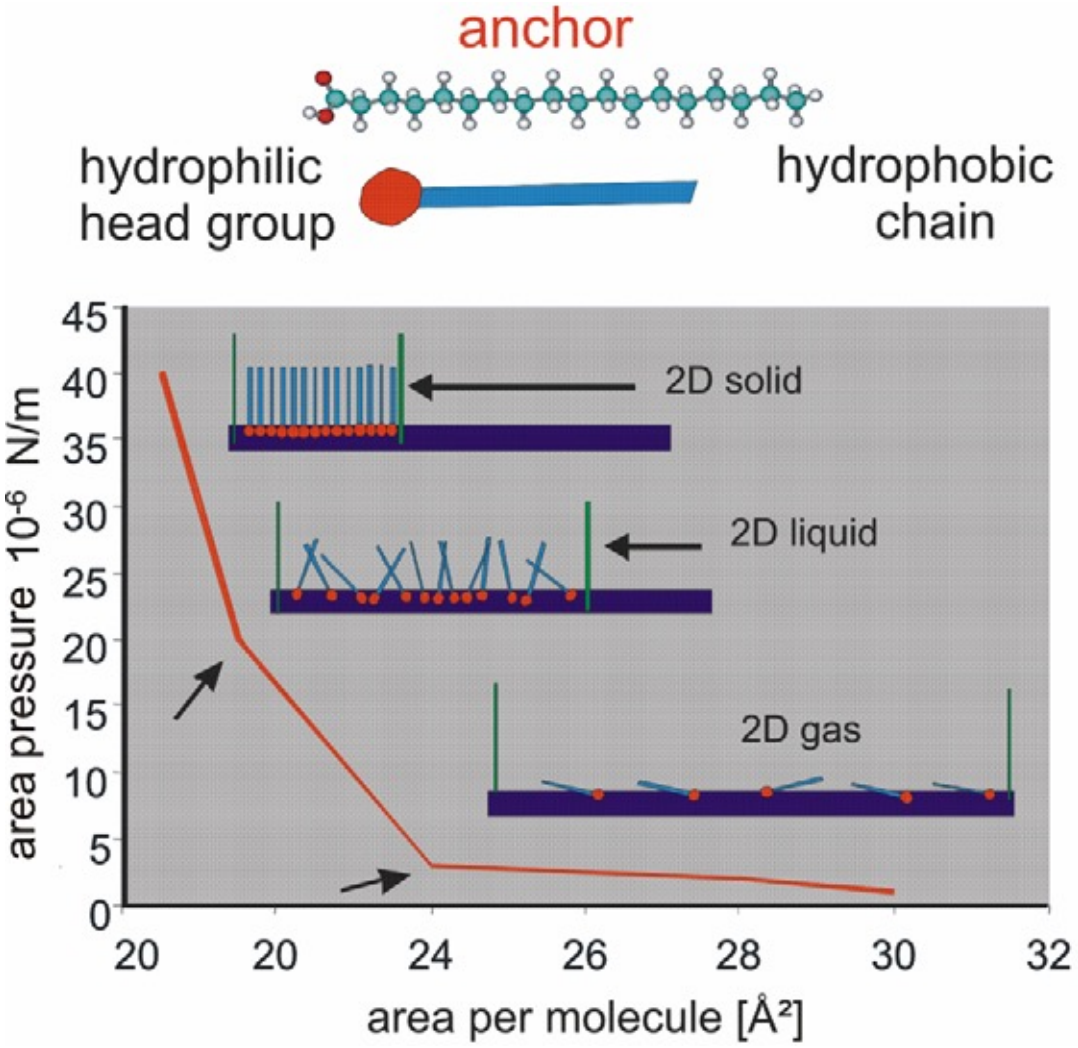

Progress in Surface Science 84 (2009) 230–278